Master's thesis

NTNU
Norwegian University of Science and Technology
Faculty of Engineering
Department of Marine Technology

Birte Larsgård Steinsvik

Autonomous Docking of Surface Vessels to Harbour using Mode-Based Hybrid Control

Master's thesis in Marine Technology
Supervisor: Asgeir J. Sørensen
June 2019

NTNU
Norwegian University of
Science and Technology

Birte Larsgård Steinsvik

Autonomous Docking of Surface Vessels to Harbour using Mode-Based Hybrid Control

Master's thesis in Marine Technology
Supervisor: Asgeir J. Sørensen
June 2019

Norwegian University of Science and Technology
Faculty of Engineering
Department of Marine Technology

NTNU
Norwegian University of
Science and Technology

NTNU Trondheim
Norwegian University of Science and Technology
Department of Marine Technology

MASTER THESIS IN MARINE CYBERNETICS

SPRING 2019

FOR

STUD. TECHN. BIRTE LARSGÅRD STEINSVIK

Autonomous Docking of Surface Vessels to Harbour using Mode-Based Hybrid Control

Work description (short description)
The docking process of a surface vessel to a harbour is a high-risk operation that demands precision and is often time strained. A problem concerning docking situations, is to unberth when the weather loads has altered while the ship was docked. In such situations, the amount of force needed for unberthing is unknown. Unberthing with less unberthing force than needed leads to the vessel being unable to unberth, and in worst case the vessel can be slammed against the quay and cause great damage. This thesis focuses on developing a docking algorithm for being able to leave the quay in changing weather, without the vessel being slammed against the quay.

Scope of work
1. Review necessary literature within the field of autonomous docking and hybrid control.
2. Develop a docking algorithm with a hybrid controller based on the current mode of the vessel – DP, berthing and unberthing. A switching logic assuring the switching between the controllers to occur without shattering shall be included.
3. Ensure the ability to leave the quay in a safe matter in changing weather.
4. Extend the simulation environment MCSim with autonomous docking possibilities, including a quay module to simulate the quay forces the vessel experience while docked.
5. Simulate relevant scenarios in Simulink to verify the system.

The report shall be written in English and edited as a research report including literature review, description of mathematical models, description of control algorithms, simulation results, discussion and a conclusion including a proposal for further work. Source code should be provided. It is supposed that Department of Marine Technology, NTNU, can use the results freely in its research work, unless otherwise agreed upon, by referring to the student's work.

The thesis should be submitted within 11th June.

Asgeir J. Sørensen

Professor Asgeir Sørensen
Supervisor

Abstract

The technology is rapidly evolving and *digitalisation* is a buzzword in all parts of the community. The maritime industry is not an exception and technological solutions are being implemented everywhere to increase efficiency and safety. The possibilities of having fully autonomous ships conducting certain operations are being explored by several companies. The challenges in autonomous shipping range from path planning and collision avoidance to autonomous docking. The docking process of a surface vessel to a harbour is a high-risk operation that demands precision and is often time strained. This master's thesis presents a mode-based hybrid control system for autonomously docking of surface vessels to harbour.

The hybrid control system consists of a controller bank with controllers corresponding to the operation use modes of DP, berthing and quayside, and unberthing. A supervisory switch system is used for switching between the controllers when the different modes are entered. Two different methods of unberthing are developed; UNB1 and UNB2. UNB1 uses the DP controller, while UNB2 uses a separate unberthing controller. For both methods, the reference model is reset in order to achieve the desired performance. The reference model is reset by implementing a secondary reference model with a set-point outside of the quay. The secondary reference model is switched to upon unberthing. For UNB2 a wind feedforward algorithm is implemented to generate enough unberthing force when wind loads act on the vessel.

A case-study is conducted to show by simulation the performance of the docking algorithm. The simulation results show the expediency of resetting the reference model for unberthing for both UNB1 and UNB2. For UNB1 the reset of the reference model gives enough unberthing force to be able to unberth rapidly, while for UNB2 the reset of the reference model ensures a smooth path. Further, the simulation results show the performance of the docking algorithm with wind applied during the vessel's time at the quayside.

During unberthing with UNB1 and wind forces applied, the performance is dependent on the distance to the quay of the secondary set-point. A set-point close to the quay creates less force than a set-point further from the quay. Hence, with wind enabled towards the quay, placing the set-point further from the quay gives the best performance.

During unberthing with UNB2 and wind forces applied, the performance is dependent on the accuracy of the wind feedforward algorithm. The simulation results compare the ability the vessel has to unberth with no wind feedforward algorithm and with a 100% accurate wind feedforward. In real life, the accuracy of the wind measurements will never be 100%. Regardless, the wind feedforward algorithm is able to alter the unberthing force to a more suiting magnitude than without the wind feedforward algorithm.

Samandrag

Teknologien utviklar seg raskt og *digitalisering* er i vinden i alle delar av samfunnet. Den maritime industrien er ikkje eit unntak, og teknologiske løysingar vert implementert overalt for å auke effektivitet og sikkerheit. Moglegheitene for å ha fullt autonome skip som utfører visse operasjonar vert forska på av fleire selskap. Utfordringane i autonom shipping varierer frå bane planlegging og anti-kollisjonssystem til autonom dokking. Dokkingsprosessen av eit overflatefartøy til ei hamn er ein høgrisikooperasjon som krev presisjon og er ofte tidsavgrensa. Denne mastergradsoppgåva presenterer eit modusbasert hybridstyringssystem for autonom dokking av overflatefartøy til hamn.

Hybridstyringssystemet består av ein bank med regulatorar som svarer til dei ulike driftsmodusane for DP, tillegging og ved kai, og frålegging. Eit rettleiingssystem er brukt til å bytte mellom regulatorane når skipet er i dei ulike modusane. To forskjellige metodar for frålegging er utvikla; UNB1 og UNB2. UNB1 bruker DP-regulatoren, medan UNB2 bruker ein separat fråleggingsregulator. For begge metodane er referansemodellen tilbakestilt for å oppnå ønska yting. Referansemodellen er tilbakestilt ved å implementere ein sekundær referansemodell med settpunkt utanfor kaia. Den sekundære referansemodellen vert bytta til i fasa for frålegging. For UNB2 er ein algoritme for forovekopling av vindkrefter implementert for å generere nok kraft til å legge frå kai i vind.

Ein case-study er utført for å vise ytinga til dokkingsalgoritmen gjennom simulering. Simuleringsresultata viser at det er hensiktsmessig å tilbakestille referansemodellen ved frålegging for både UNB1 og UNB2. For UNB1 gir tilbakestillinga av referansemodellen nok fråleggings kraft for å kunne legge frå raskt, medan for UNB2 sikrar tilbakestillinga av referansemodellen ei jamn bane. Vidare viser simuleringsresultata korleis dokkingalgoritmen yter når vind er påført medan skipet ligg til kai.

Under frålegging med UNB1 og påførte vindkrefter, er ytinga avhengig av avstanden mellom kaia og sekundær settpunktet. Eit settpunkt nær kaia skaper mindre kraft enn eit settpunkt lenger vekk frå kaia. Derfor, med vind aktivert mot kaia, gir plassering av settpunktet lenger frå kaia den beste ytinga.

Under frålegging med UNB2 og påførte vindkrefter, er ytinga avhengig av nøyaktigheita av foroverkopliga av vindkreftene. Simuleringsresultata samanliknar evna fartøyet har til å legge frå kai med og utan foroverkopling av vindkrefter, der foroverkoplinga er 100% nøyaktig. I røynda vil nøyaktigheita av vindmålingane aldri være 100%. Uansett, er algoritmen for foroverkopling av vindkrefter i stand til å endre fråleggings-krafta til ein meir passande storleik enn utan foroverkoplinga.

Preface

This thesis is written at the Department of Marine Technology at the Norwegian University of Science and Technology during the spring of 2019 and concludes my five years of studying in Trondheim.

I have since the 3rd grade, back in 2016, had a wish to work with autonomous ships - which was the reason why I chose to specialize in Marine Cybernetics. During the work of this thesis I have been able to delve into the depth of the autonomous docking process and look at one of the challenges; unberthing without slamming against the quay. The work of this thesis has been both challenging and educational, the goal has not always been clear and the product is not what was anticipated when I started working with the thesis in January. There have been many times of confusion, and one of my favourite quotes from my supervisor is quite descriptive; *"Still confused? But on a higher level!"*.

I would like to express my gratitude to my supervisor, Professor Asgeir J. Sørensen. No question has ever been too stupid and he always made sure I understood what he was trying to explain. Not only did he give me professional advice about the thesis, but he has also been a great support during tough periods and encouraged me in times of self-doubt.

A huge thanks goes to all involved in the development of the simulation environment MCSim over the years. Especially to Astrid Brodtkorb, who has kindly answered questions about how the simulator behaves.

I would like to thank my family for the love and support they have given throughout my five years of studying marine technology. Thanks to my fellow students and office mates for all the good times we have had. It can be hard to be a student sometimes and it is nice to know that you are not alone. Last but not least, I would like to thank my dear friend Elizabeth M. Møller for proofreading.

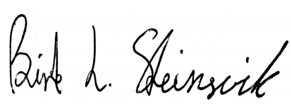

Birte Larsgård Steinsvik
Trondheim, 11.06.19

Table of Contents

List of Tables

List of Figures

Abbreviations

AUV	=	Autonomous Underwater Vehicle
CS3	=	Cybership 3
CoG	=	Center of Gravity
DOF	=	Degrees of Freedom
DP	=	Dynamic Positioning
LF	=	Low-Frequency
MCLab	=	Marine Cybernetics Laboratory
MCSim	=	Marine Cybernetics Simulator
NED	=	North-East-Down
PID	=	Proportional-Integral-Derivative
PSV	=	Platform Supply Vessel
SW1	=	Switching Criteria 1
SW2	=	Switching Criteria 2
UNB1	=	Unberthing Method 1
UNB2	=	Unberthing Method 2
USV	=	Unmanned Surface Vessel
WF	=	Wave-frequency

Chapter 1

Introduction

1.1 Background and Motivation

Exiting developments are happening in the autonomous technology, and an increasing amount of companies are exploring the possibilities for autonomous ships. Some recent examples of such companies are DNV GL with the research project ReVolt (DNV GL 2018), Kongsberg with the container ship Yara Birkeland (Stensvold 2017), and NTNU with the passenger ferry Milliampere (Skoglund 2018). Autonomous vessels can improve the shipping industry as we know it today with regards to efficiency and safety. Thus there is reason to believe that in the future, ships will no longer be steered by humans. However, for autonomous ships to be able to execute operations in a safe and efficient manner, several challenges must be met.

The challenges in autonomous shipping range from path planning and collision avoidance to autonomous docking. There are several studies in the literature about these challenges, as Bitar (2017) enlightened. When it comes to autonomous docking there are numerous examples of AUV and USV docking, less research have been done on harbour docking. With limited papers published on the field, the study of autonomous docking of surface vessels to harbour becomes both more interesting and more challenging.

Autonomous docking was an addressed problem already in the early 90s, and a fuzzy logic control system is described by Rae et al. (1993). This method allows an AUV to be safely docked with another moving AUV, by recursively driving the docking vehicle in an increasingly better position for docking. The fuzzy method is a set of rules that alters the course of the AUV when moving. The speed of the AUV is decreased with the distance to the target, and when the final target is reached, the AUV is docked. Another docking algorithm using fuzzy logic is presented in Teo et al. (2015). The paper claims to have performed the first sea trials on underwater AUV docking using fuzzy-based docking methodology with real-time implementation. In this case the docking station is under water and stationary.

Even if there is little to no publications on fully autonomous docking of ships to harbours, there are several recent examples from the industry where autonomous docking is performed. The theme is indeed relevant for shipping in near future. In the spring of 2018 Wärtsila sucessfully tested their autodocking system on a Norwegian ferry, Folgefonn (Wärtsila Corporation 2018). According to Wärtsila, the system performed a fully autonomous docking, including transit, gradual slowing of speed and finally docking. 8 months later, Rolls-Royce and Finferries successfully demonstrated their fully autonomous ferry, Falco (Rolls-Royce 2018). In addition to perform a fully autonomous crossing and docking, Falco also detected objects and conducted collision avoidance. Figure 1.1 shows Falco under transit.

Figure 1.1: The Rolls-Royce and Finferries developed autonomous ferry, Falco ©Rolls-Royce.

The docking process of a surface vessel to a harbour is a high risk operation that demands precision, and is often time strained. The docking process starts when the vessel is in a suitable distance to the quay, and the phase of slow speed is entered. For non-autonomous vessels the captain or mate take manually control of the ship and steers the ship to quay, as it is difficult for the auto-pilot to control the ship with little thrust. The way the docking is executed is dependent on the type of ship, the design of the quay, and the personal preference of the captain. For overactuated vessels, such as supply vessels and some ferries, the ship is maneuvered until it is parallel with the quay before a force is applied so that the vessel is parallel shifted towards the quay. For underactuated vessels, for example freighter ships, it is common to first maneuver the bow to the quay and then use the rudder and main propeller at the stern to move the stern of the ship against the quay. (Steinsvik 2019*b*)

After the vessel's task at quay is performed, the docking operation continues with the unberthing of the vessel and finally leaving the quay. For a vessel to be fully autonomous, it needs to be able to handle different operations and adjust for all kinds of weather. This is especially an issue when berthing and unberthing, as high precision is demanded. It is not accepted for the vessel to suddenly move several metres out of path - as this may lead to collision with the quay. To be able to handle the changes of operations and weather a hybrid control system structure can be utilised. Hybrid control systems are widely described in the literature by i.e. Hespanha (2001). The use of hybrid control for surface vessels described in the literature mainly concerns dynamic positioning (DP) in varying sea states e.g. the works of Nguyen et al. (2007), Hassani et al. (2012) and Brodtkorb (2017). The use of hybrid control in docking of autonomous vessels to harbour is on the other hand less documented. The aim of this thesis is to present a design of a hybrid control system used for docking of surface vessels to harbour.

1.2 Research Questions and Objectives

The main research questions of this thesis is:

How can the docking process of a surface vessel be performed autonomously in a good manner? Is it possible to develop some unberthing control ensuring the vessel to leave the quay rapidly, to avoid the possibility of slamming against the quay upon leaving? Possible weather changes during the time the vessel is at quayside should be considered.

In order to be able to answer the research questions, the objectives of this thesis are as following

- Do a literature review of autonomous docking and hybrid control.
- Get familiar with the simulation environment MCSim.
- Design a hybrid controller for autonomous docking.
- Develop some unberthing algorithm generating enough force for unberthing.
- Expand MCSim for autonomous docking with a hybrid controller.
- Perform a case-study to verify the system performance.

1.3 Contributions

In this thesis a hybrid controller for autonomous docking is developed. The hybrid controller consists of controllers for the following operation modes: DP, berthing and quayside, and unberthing. The controller is taking into account the possibilities of drastically changes of weather. The simulation environment MCSim has been altered for simulating docking events, including implementation of a quay module and the hybrid control system.

1.4 Thesis Outline

Chapter 2 - Mathematical Models: Presents mathematical models for marine surface vessels and control models and controllers commonly used for control of marine surface vessels.

Chapter 3 - Hybrid Control System for Marine Surface Vessels: Presents the theoretical concept of hybrid control. A hybrid control system structure and a modelling framework is shown. The concept of supervisory switching is described.

Chapter 4 - Development of the Docking Algorithm: Presents the full docking algorithm, from DP to quay to DP. The relevant modes of operation are described. The different controllers and the switching logic are explained. The features of resetting the reference model and wind feedforward control is described.

Chapter 5 - Case-Study: Presents a case-study. The simulation environment is briefly described. The characteristics of the vessel used for simulation are presented. Some tuning parameters are discussed, and simplifications are stated. Finally the simulation results are presented and briefly discussed.

Chapter 6 - Discussion: Gives a further discussion of the simulation results. Additionally, improvements and limitations are discussed.

Chapter 7 - Conclusions and Further Work: Concludes the thesis and suggest further work.

Chapter 2

Mathematical Models

This chapter aims to provide the necessary theoretical foundation for how marine surface vessels are modelled and controlled. The theory presented here is retrieved from Fossen (2011) and Sørensen (2018), the reader is referred to study these references for detailed explanations. Except for Section 2.1.4, which is developed for the purpose of this thesis.

2.1 Modelling of Marine Surface Vessels

2.1.1 Reference Frames

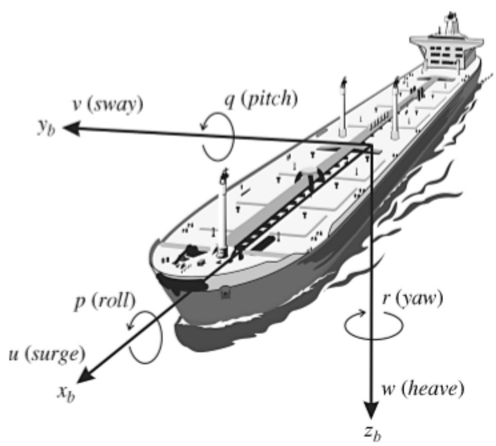

Figure 2.1: 6 DOF motions for surface vessels in the body-fixed reference frame (Fossen 2011).

The reference frames used are the North-East-Down (NED) and the body-fixed reference frames. Figure 2.1 shows the 6 DOF motions in the body-fixed reference frame and Figure 2.2 shows the relations between the frames.

- The NED frame is a local reference frame used for position and distance. With the use of NED, the x-axis points towards true north, the y-axis points towards east and the z-axis points towards the Earth's centre.
- The body-fixed frame is fixed to the vessel body with origin usually placed along the vessels centreline in the waterline. With the use of a body-fixed reference frame, the x-axis points towards the bow, the y-axis points towards starboard and the z-axis points down.

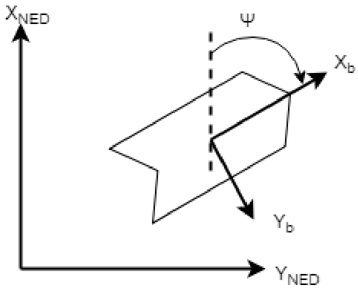

Figure 2.2: Relation between the NED frame and the body-fixed frame.

2.1.2 Transformation between BODY and NED

Positions $\boldsymbol{\eta}$ and distances are given in the NED frame, while force working on the vehicle $\boldsymbol{\tau}$ and velocity $\boldsymbol{\nu}$ is given in the body-fixed frame. To be able to give appropriate force depending on the distance to the quay, a transformation from NED to body is necessary. The transformation is performed by rotating the vectoral distance from NED frame to body frame through a rotation matrix, $\boldsymbol{R}(\psi)$, as shown in (2.1). As only the horizontal plane is considered, the 3 DOF rotation matrix is applied.

$$\tilde{\boldsymbol{\nu}}^b = \boldsymbol{R}(\psi)\tilde{\boldsymbol{\nu}}^{NED} \tag{2.1}$$

$\tilde{\boldsymbol{\eta}}^b$ is the difference of the vessels position and the desired position in body frame, $\tilde{\boldsymbol{\nu}}^{NED}$ is the distance in NED frame and $\boldsymbol{R}(\psi)$ is the rotation matrix defined as

$$\boldsymbol{R}(\psi) = \begin{bmatrix} cos(\psi) & -sin(\psi) & 0 \\ sin(\psi) & cos(\psi) & 0 \\ 0 & 0 & 1 \end{bmatrix} \tag{2.2}$$

where ψ is the heading of the vessel, and thus the difference between the NED and body frame, as can be seen in Figure 2.2.

2.1.3 Vessel Dynamics

The total vessel dynamics can be modelled by a low-frequency (LF) model and a wave-frequency (WF) model, as shown in Figure 2.3. The LF motions caused by mean wind, current and second-order wave forces can be separated from the WF motions caused by first-order wave loads. As the mean of the first-order wave loads is equal to zero, these loads are filtered out with a wave filter to reduce unnecessary wear and tear on the actuators.

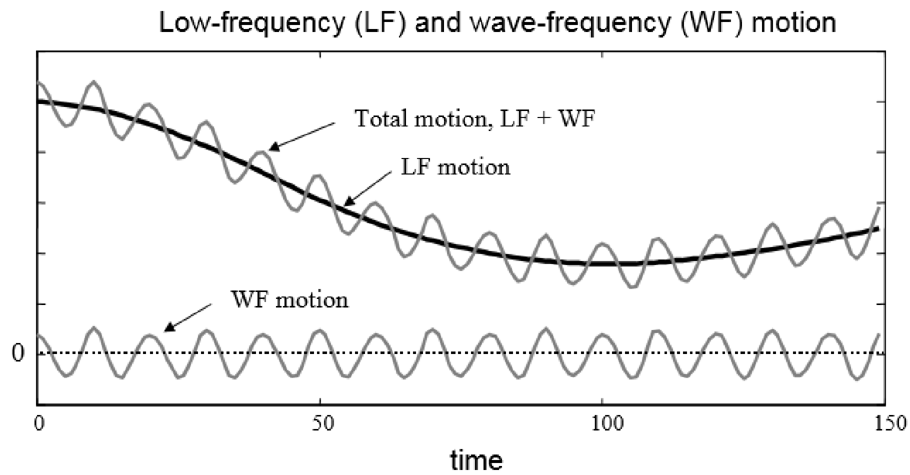

Figure 2.3: Total vessel dynamics modeled by a LF model and a WF model (Sørensen 2018).

The nonlinear body-fixed 6 DOF equation of motion is written as follows (Fossen 2011)

$$\dot{\boldsymbol{\eta}} = \boldsymbol{J_\theta}(\boldsymbol{\eta})\boldsymbol{\nu} \tag{2.3}$$

$$\boldsymbol{M}\dot{\boldsymbol{\nu}} + \boldsymbol{C}_{RB}(\boldsymbol{\nu})\boldsymbol{\nu} + \boldsymbol{C}_A(\boldsymbol{\nu}_r)\boldsymbol{\nu}_r + \boldsymbol{D}(\boldsymbol{\nu}_r)\boldsymbol{\nu}_r = \boldsymbol{\tau} + \boldsymbol{\tau}_{env} \tag{2.4}$$

where $\boldsymbol{\eta} \in \mathbb{R}^{6\times1}$ is the position and orientation in NED, $\boldsymbol{\nu} \in \mathbb{R}^{6\times1}$ is the linear and angular velocities in the body-fixed frame, $\boldsymbol{J_\theta} \in \mathbb{R}^{6\times6}$ is a transformation matrix, mapping velocities from body to NED frame. $\boldsymbol{M} = \boldsymbol{M}_A + \boldsymbol{M}_{RB}$ is the mass matrix, $\boldsymbol{C}$ is the Coriolis and centripetal matrix, $\boldsymbol{D}$ is the damping matrix and $\boldsymbol{\tau}$ is the thruster force and $\boldsymbol{\tau}_{env}$ is the environmental forces from wave, wind and current loads. Subscript A is added mass, while subscript RB is rigid-body.

For conventional surface vessels, only 3 degrees of freedom are considered; surge, sway and yaw. Dynamics associated with motions in heave, roll and pitch are neglected, and the state vectors are chosen as $\boldsymbol{\eta} = [N, E, \psi]^T$ and $\boldsymbol{\nu} = [u, v, r]^T$. The general 6 DOF equation is reduced to a 3 DOF by reducing the 6 DOF transformation matrix $\boldsymbol{J_\theta}(\eta)$ to the 3 DOF transformation matrix $\boldsymbol{R}(\psi)$.

Under the assumption of low speed, the Coriolis and centripetal forces are negligible and the linear damping term dominates, such that the 3 DOF low-speed model can be written as shown in (2.5) - (2.7). For details see Fossen (2011) and Sørensen (2018).

$$\dot{\boldsymbol{\eta}} = \boldsymbol{R}(\psi)\boldsymbol{\nu} \tag{2.5}$$

$$\boldsymbol{M}\dot{\boldsymbol{\nu}} + \boldsymbol{D}\boldsymbol{\nu} = \boldsymbol{R}^T(\psi)\boldsymbol{b} + \boldsymbol{\tau}_{env} \tag{2.6}$$

$$\dot{\boldsymbol{b}} = \boldsymbol{0} \tag{2.7}$$

2.1.4 Quay Model

A vessel that is docked to a quay will experience the force from the quay to be of equal magnitude as the vessel is exerting on the quay, according to Newtons 2nd law. Delays in the model leads to a simulation problem when modelling the force from the quay to be of the same magnitude as the force from the vessel; the vessel is able to move beyond the quay. This is avoided by modelling the force from the quay as a step function

$$\boldsymbol{\tau}_q = \left\{ \begin{array}{cc} 0 & \boldsymbol{\eta} < \boldsymbol{\eta_q} \\ 0.5\boldsymbol{F_q} & \boldsymbol{\eta} = \boldsymbol{\eta}_q \\ \boldsymbol{F_q} & \boldsymbol{\eta} > \boldsymbol{\eta_q} \end{array} \right\} \tag{2.8}$$

where $\boldsymbol{\tau}_q$ is the force acting on the vessel from the quay, $\boldsymbol{\eta}$ is the vessel position and $\boldsymbol{\eta}_q$ is the quay position. The quay force $F_q^N \approx \infty$ is set to be 10 times the maximal force of the thrusters.

As forces are given in the body-frame, while the quay forces always will be perpendicular to the quay, a rotation of the quay-forces must be performed. This is ensured by implementing (2.9) and (2.10)

$$F_q^b(1) = \underbrace{F_q^N(1)cos(\beta_1 - \psi)}_{\text{For } \boldsymbol{\eta}(1) >= \eta_q(1)} + \underbrace{F_q^N(2)cos(\beta_2 - \psi)}_{\text{For } \boldsymbol{\eta}(2) >= \eta_q(2)} \tag{2.9}$$

$$F_q^b(2) = \underbrace{F_q^N(1)sin(\beta_1 - \psi)}_{\text{For } \boldsymbol{\eta}(1) >= \eta_q(1)} + \underbrace{F_q^N(2)sin(\beta_2 - \psi)}_{\text{For } \boldsymbol{\eta}(2) >= \eta_q(2)} \tag{2.10}$$

where F_q^b is the quay force in the body-fixed frame, F_q^N is the quay force in the NED frame, β_1 and β_2 are the angles of the quay forces in NED x- and y- directions respectively, and with $\beta_2 = \beta_1 + \pi/2$. Figure 2.4 shows the quay forces working on the vessel, with $\beta = [0, \pi/2]^T$. For most cases, the desired docking angle is $\psi = \beta_1$ or $\psi = \beta_2$. The figure shows the vessel tilted relative to the quay, to demonstrate the forces from quay working perpendicular to the quay in the NED frame.

From the Figure, the forces from the quay is pointing towards the CoG of the vessel, hence in opposite direction of the body-fixed frame as seen in Figure 2.2. In the simulation, this leads to a subtraction of the quay force.

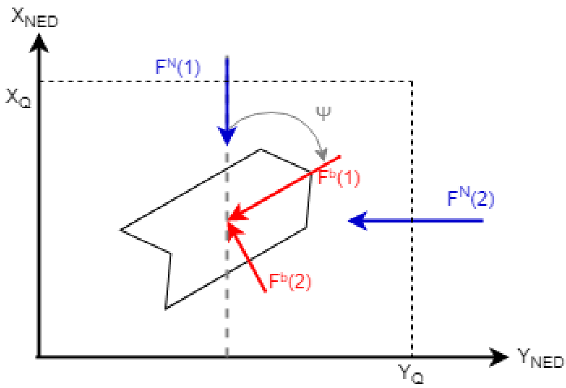

Figure 2.4: Quay forces working on the vessel when the vessel is at quayside. The blue arrows are the forces acting from the quay in NED-frame while the red arrow shows the forces in the body-fixed frame. The stippled lines are the quay axes. Here the angles of the quay forces are $\beta = [0, \pi/2]^T$

2.2 Control of Marine Surface Vessels

This section briefly describes some control models and controllers commonly used for control of marine surface vessels. One controller for transit and one controller for DP are presented here.

2.2.1 Transit Control

For autonomous ships in transit, an autopilot is used to control the heading of the vessel. The autopilot is a PID controller based on the first-order Nomoto model. The Nomoto model can be derived from a linearization of (2.3) and (2.4), and is obtained by neglecting the second order dynamics. The first-order Nomoto model can be approximated as

$$T\ddot{\psi} + \dot{\psi} = K\delta \tag{2.11}$$

where T is a time constant, ψ is the heading of the vessel, K is the rudder constant and δ is the rudder angle. A detailed derivation of both first- and second-order Nomoto model can be studied in Fossen (2011).

With the deviation $\tilde{\psi}$ expressed as in (2.12), where ψ_d is the desired heading and ψ is the actual heading, the 1 DOF PID controller based on the Nomoto model is shown in (2.13) below. K_p, K_d and K_i are the controller gains for the proportional, derivative and integral terms respectively.

$$\tilde{\psi} = \psi - \psi_d \tag{2.12}$$

$$\tau_N = -K_p\tilde{\psi} - K_d\dot{\tilde{\psi}} - K_i \int \tilde{\psi} dt \tag{2.13}$$

2.2.2 DP Control

When approaching the quay, it is suitable to switch from autopilot control to dynamic positioning (DP) control. A DP controller can be seen as an extended autopilot model, where the position in x- and y-direction are controlled in addition to the heading ψ. The DP model is a 3 DOF model and is valid for station keeping and low-speed manoeuvring, with a velocity up to 2 m/s (Fossen 2011). Concerning 3 DOF, $\boldsymbol{\eta} = [x, y, \psi]^T$ and $\boldsymbol{\nu} = [u, v, r]^T$ are the position and velocity state vectors.

Expressing the position deviation $\tilde{\boldsymbol{\eta}}$ in the body-fixed frame as in (2.14) and the velocity deviation $\tilde{\boldsymbol{\nu}}$ as in (2.15), a 3 DOF PID controller as shown in (2.16) can be used for DP control. For a faster response, a feedforward controller as shown in (2.17) can be implemented in addition to the PID. Here $\boldsymbol{D}$ is the linear damping matrix and $\boldsymbol{M}$ is the mass matrix. The total DP controller is displayed in (2.18).

$$\tilde{\boldsymbol{\nu}} = \boldsymbol{R}^T(\psi_d)(\boldsymbol{\eta} - \boldsymbol{\eta_d}) \tag{2.14}$$

$$\tilde{\boldsymbol{\nu}} = \boldsymbol{\nu} - \boldsymbol{\nu_d} \tag{2.15}$$

$$\boldsymbol{\tau}_{PID} = -K_p\tilde{\boldsymbol{\nu}} - K_d\tilde{\boldsymbol{\nu}} - K_i \int \tilde{\boldsymbol{\nu}} dt \tag{2.16}$$

$$\boldsymbol{\tau}_{ff} = \boldsymbol{D}\tilde{\boldsymbol{\nu}} + \boldsymbol{M}\dot{\tilde{\boldsymbol{\nu}}} \tag{2.17}$$

$$\boldsymbol{\tau}_{DP} = \boldsymbol{\tau}_{PID} + \tau\tau_{\tau_{\tau_{ff}}} \text{(2.18)}$$

Reference Model

To ensure a smooth transition to the desired position when using PID control it is common to implement a reference model. The reference model creates a path to be followed, hence the desired position $\boldsymbol{\eta}_d$ is changing over time, leading to a smaller distance between the vessel position $\boldsymbol{\eta}$. Less difference between $\boldsymbol{\eta}$ and $\boldsymbol{\eta}_d$ leads to a slower, but more controlled use of PID. The effect is reduced integral wind-up and a gentler use of the actuators.

For control of marine vessels it is suitable to use a reference model based on a mass-damper-spring system cascaded with a low-pass filter. Such reference models can be illustrated by (2.19) (Fossen 2011)

$$h(s) = \frac{\eta_{d_i}}{r_i}(s) = \frac{\omega_{n_i}^3}{(s + \omega_{n_i})(s^2 + 2\zeta_i\omega_{n_i}s + \omega_{n_i})}, i = (1, 2, 6) \tag{2.19}$$

where $\boldsymbol{\eta}_{d_i}$ is the desired position at each timestep, r_i is the final position, ζ_i is relative damping ratio, and ω_{n_i} is natural frequency. $i = (1, 2, 6)$ indicates the different states in the horizontal plane; surge, sway and yaw. The reference model is presented as a block diagram in Figure 2.5.

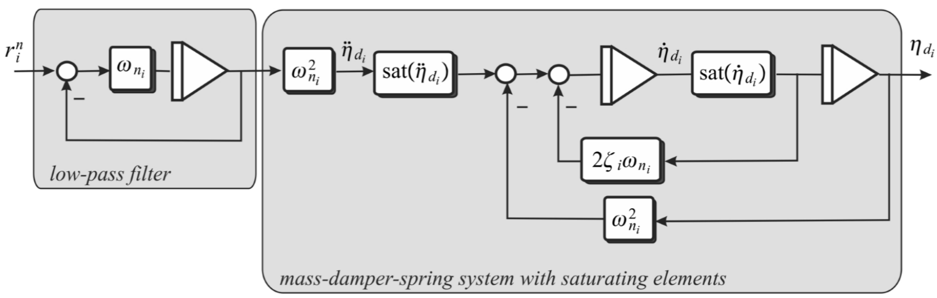

Figure 2.5: Block diagram for a reference model based on a mass-damper-spring system cascaded with a low-pass filter (Fossen 2011).

Chapter 3

Hybrid Control System for Marine Surface Vessels

3.1 Introduction to Hybrid Control

A simple controller is only valid and usable in operations and conditions it is designed and tuned for. In the real world, situations where the conditions change due to the environment and modes of operation, are more common than not. Therefore, it is advantageous to be able to switch between different controllers designed for different conditions or operations. Systems with multiple controllers and the ability to switch between these are called hybrid control systems. Hybrid control systems combines continuous dynamics with discrete logic. Several different controllers designed for different purposes can be switched between automatically, increasing the system reactivity, efficiency and safety of any operation, compared to commonly used ad-hoc methods for phasing in and out controllers based on an operator changing the use mode and vessel speed (Sørensen 2018). In autonomous docking it is expedient to use hybrid controllers since both conditions and operations vary throughout the process.

Hybrid control for docking of autonomous surface vessels is not widely found in the literature. However, some relevant work is done on hybrid control for dynamic positioning (DP). In Nguyen et al. (2007) , a hybrid controller for DP is designed with the ability to withstand different sea states from calm water to extreme seas. The work of Nguyen et al. (2007) is based on Hespanha (2001), Hespanha & Morse (2002) and Hespanha et al. (2003). An estimator-supervision system is used, comparing the behaviours of some models and the actual process. The model that best describes the ongoing process is chosen.

Figure 3.1 shows the different operation conditions for marine surface vessels; speed of the vessel, environment and use mode. In addition to the operation conditions shown in the figure, loading condition has an impact. These conditions indicate the performance of the vessel during various tasks, with varying speed in an uncertain and changing environment (Sørensen 2018). Hybrid control systems for marine surface vessels are often designed to be able to manage changes in operational conditions, whether it is concerning changes in the environment, speed, loading condition, use mode, or a combination of these.

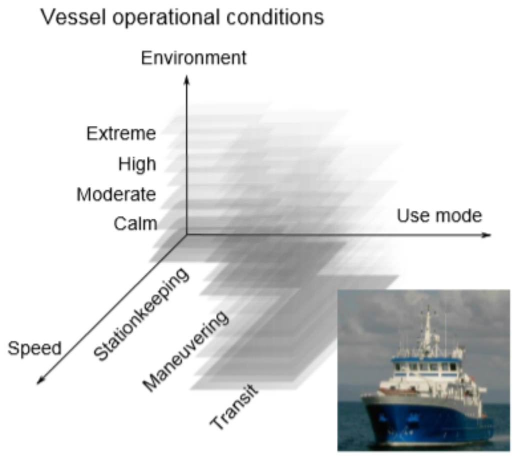

Figure 3.1: Operational conditions for surface vessels: use mode, speed and environment (Sørensen 2018).

The hybrid control systems developed in the works of Nguyen et al. (2007), Brodtkorb (2017), and Hassani et al. (2012) are all built to handle different environmental conditions, from calm sea to extreme weather. Common for hybrid control systems built to be able to handle different sea conditions, is that in the controller bank, a controller for each sea state is present. The switching between these controllers are based on the sea condition at each instant of time. Hence, the environmental conditions from Figure 3.1 is considered.

Some work exists on autonomous docking using hybrid control for non-marine vessels, particularly in combination with visual feedback. In Amarasinghe et al. (2005), a mobile robot is autonomously docked, using vision-based hybrid control strategy. The controllers in this system are designed for different states; start, forwards, backwards and stop. From the operational conditions for surface vessels in Figure 3.1, one can compare the states for the docking of the mobile robot with the use mode, giving an example of a hybrid control system where the use mode is considered.

3.2 Hybrid Control System Structure

A hybrid control system consists of several different control systems and a supervisor that switches between the different systems, to ensure that the most suitable system is in action at each instant of time. The complexity of the systems varies. One can design hybrid systems that involves multiple full systems consisting of observers, controllers, control allocation and actuator controllers. Less complex systems can for instance only switch between multiple controller candidates, while the rest of the system is kept constant.

Figure 3.2 shows the structure of a hybrid control system with a bank of observer candidates and a bank of corresponding controller candidates. The model is from the work of Nguyen et al. (2007) on hybrid control for DP in different sea conditions. As this hybrid controller system is designed for different sea states, both different observers and controllers are needed. For a docking situation it is sufficient to use the same observer throughout the docking phase, but the need of several observers will rise in combination with a transit controller.

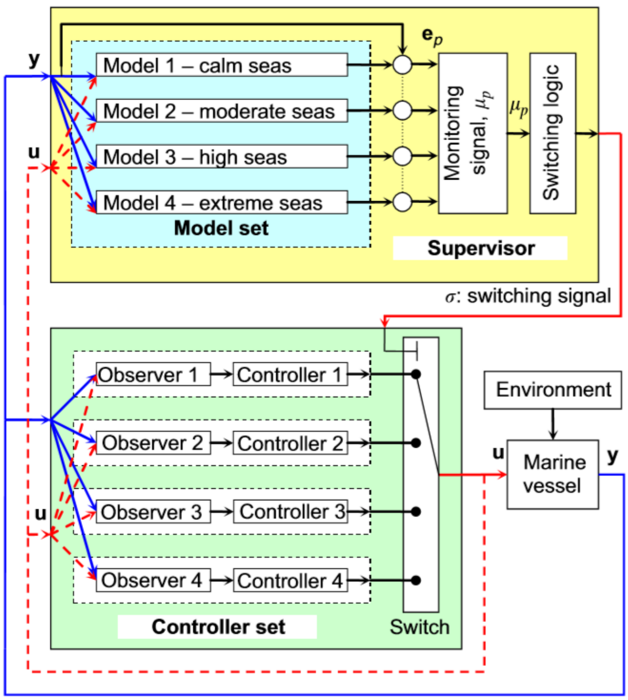

Figure 3.2: Structure of a estimator-based hybrid control system for DP in changing environmental conditions (Nguyen et al. 2007).

3.3 Modelling Framework

There exists several mathematical frameworks for modelling of hybrid system. In this section the modelling framework from Goebel et al. (2012) is presented. Goebel et al. focused on the data structure and on modelling when developing the framework, creating a general framework that can be used for various hybrid systems. The framework is modelled as a differential inclusion $\dot{x} \in F(x)$, and a difference inclusion $x^+ \in G(x)$ such as

$$\begin{aligned} x \in \boldsymbol{C} \quad & \dot{x} \in F(x) \\ x \in \boldsymbol{D} \quad & x^+ \in G(x) \end{aligned} \tag{3.1}$$

x is the state of the hybrid system and can consist of states changing in continuous time, logic variables and variables that changes both in continuous and discrete time. $\boldsymbol{C}$ denotes the flow set in which the state is changing in time according to the differential inclusion $\dot{x} = f(x)$ for $f \in F$. $\boldsymbol{D}$ is the jump set in which the state is allowed to change instantaneously according to the difference inclusion $x^+ = g(x)$ for $g \in G$. The notation $\dot{x}$ represents the change in the state over time, velocity, while x^+ denotes the state after an instantaneous change. For details and examples of application, see Goebel et al. (2012).

3.4 Supervisory Switch Control

Hybrid control systems using switching logic to switch between controllers are called supervisory control, as the switching logic acts as a supervisor on what controller to be enabled at each instant of time. Figure 3.3 shows the concept of supervisory switching where the supervisor provides a switching signal σ. The switching signal is defined in the supervisor based on the available measurements and some switching logic.

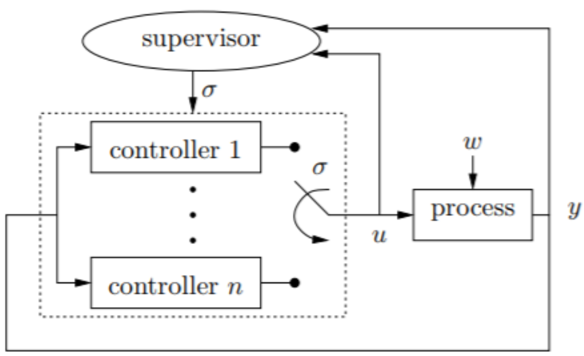

Figure 3.3: Concept of suprvisory switching control (Hespanha 2001).

Hespanha (2001) presents four essential properties for the supervisory switch control; properties of *matching*, *detectability*, *small error*, and *non-destabilization*. The properties of matching and detectability are important for understanding the overall system, while the properties of small error and non-destabilization must be satisfied by the switching logic.

The matching property is important for the multi-estimator in an estimator-based supervisory system. It states that the multi-estimator should be designed such that each estimate $\hat{y}$ provides a good approximation to the output y. The detectability property is important for the multi-controller and states that for every fixed estimator, the switched system must be detectable with the respect to the estimation error $\hat{e}$ when the signal is frozen.

The small error property makes sure that the selected controller is the most fitting at each instant of time. In cases where the process is in states where two or several controllers could be chosen, fast switching (chattering) may occur. Chattering is unwanted as it affects the stability of the switched system. The non-destabilization property both preserves the detectability and prevents chattering, by providing switching logic, such as dwell-time switching logic and hysteresis switching logic. A brief description of the dwell-time and scale-independent hysteresis switching logics follows. For a detailed explanation on both the switching properties and logics, the reader is recommended to study the tutorial on supervisory control by Hespanha (2001) and the references therein.

Dwell-time Switching Logic

Dwell-time switching logic is to dwell for a predetermined amount of time for each switch until the next switch can be carried out. Figure 3.4 shows a simplified version of the dwell-time logic. μ_p is a monitoring signal defined by (3.2),

$$\mu_p(t) = \int_0^t e^{-2\lambda(t-\tau)} \|\mathbf{e}_p(\tau)\|^2 d\tau, \qquad p \in \mathscr{P}, \tag{3.2}$$

where λ is a constant non-negative forgetting factor, $\|\mathbf{e}_p\|$ is the norm of the estimation error $\mathbf{e}_p$. The output of arg min μ_p is the index of the minimum values in the vector μ_p. (Hespanha 2001)

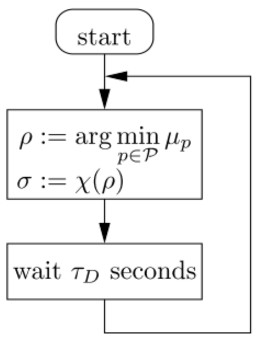

Figure 3.4: Concept of dwell-time switching logic (Hespanha 2001).

Hysteresis Switching Logic

Hysteresis switching logic slows down the switching based on the growth of the estimation errors. Figure 3.5 shows the concept of scale-independent hysteresis switching logic, where h is a positive hysteresis constant, μ_p is a monitoring signal defined by (3.3),

$$\mu_p(t) = \epsilon + e^{-\lambda t}\epsilon_0 + \int_0^t e^{-2\lambda(t-\tau)}\|\mathbf{e}_p(\tau)\|^2 d\tau, \qquad p \in \mathscr{P}, \tag{3.3}$$

where λ is a constant non-negative forgetting factor, and $\|\mathbf{e}_p\|$ is the norm of the estimation error $\mathbf{e}_p$. The output of arg min μ_p is the index of the minimum values in the vector μ_p. (Hespanha 2001)

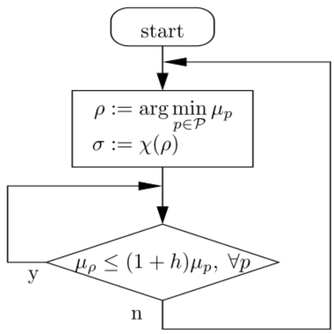

Figure 3.5: Concept of scale-independent hysteresis switching logic (Hespanha 2001).

Chapter 4

Development of the Docking Algorithm

This chapter presents the development of a docking algorithm for surface vessels. The docking algorithm consist of a hybrid control system with switching based on the current use mode.

4.1 System Overview

The hybrid controller presented in this thesis consists of a bank of three controllers. Each controller is designed to handle the different stages of the docking process; DP, berthing, unberthing and DP again. Two different methods of unberthing are developed, UNB1 and UNB2, and are described in Section 4.2.3. Figure 4.1 shows the stages of docking, and what controller is enabled at each stage. In the figure, the red dotted line corresponds to the unberthing using UNB1, while the blue line corresponds to unberthing using UNB2. Further descriptions of the different use modes and corresponding controllers are given in Section 4.2.

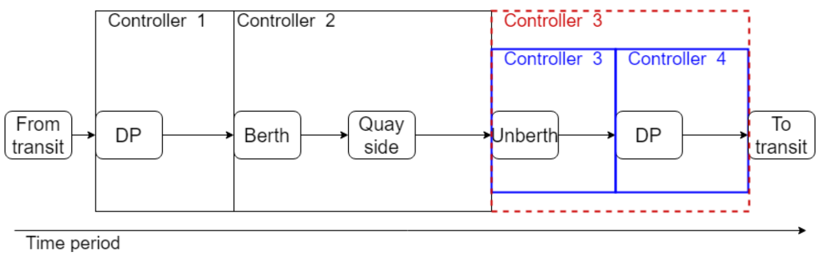

Figure 4.1: Use modes with corresponding controllers for UNB1 (dotted red line) and UNB2 (blue lines).

A reset of the reference model is necessary for both the unberthing methods. An in-depth explanation of the resetting of the reference model is given in Section 4.3. For UNB2, a wind feedforward algorithm is implemented, described in Section 4.5. The tuning of the system is described in Section 5.1.3.

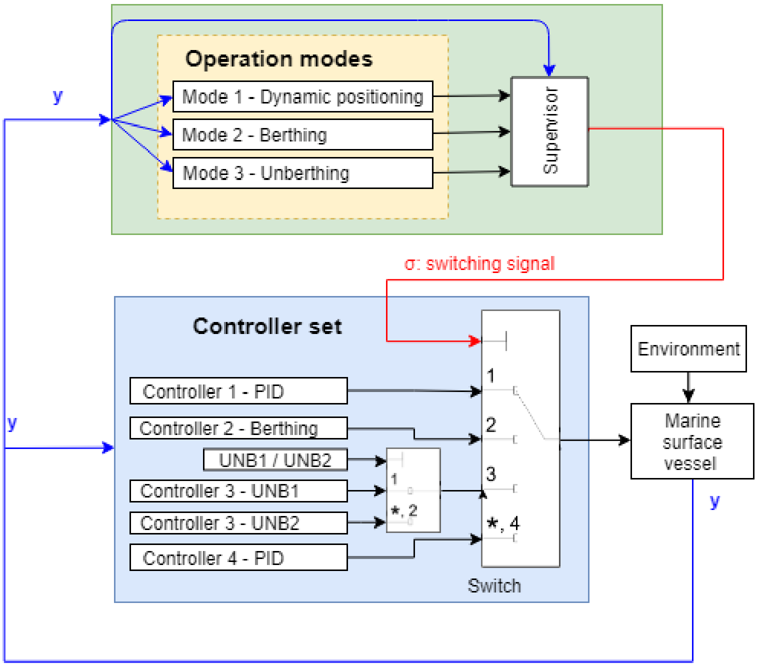

Figure 4.2: Concept of hybrid control system with discrete switching signal based on the operation modes.

As only low-speed manoeuvring is considered, the observer is consistent throughout the docking process and the supervisor is not estimator-based. This is in contrast to the hybrid controllers for DP operations discussed in Section 3.1. The switching logic is based on the current operation use mode. Figure 4.2 shows the structure of the hybrid control system. Chattering is avoided by strictly switching only from one controller to the next in a chronological matter. The supervisory switching is described in Section 4.4.

4.2 Operation Modes and Corresponding Controllers

In this section the different operation modes and the associated controllers are presented and discussed. The first two controllers in the system, the controllers for DP and berthing, are the same for both unberthing methods. The differences approach in the unberthing phase. Table 4.1 gives an overview of the controllers and for what mode they are enabled.

Table 4.1: Overview of controllers and area of application.

Nr.	Unberthing method	Controller type	Mode of application
1	UNB1 and UNB2	PID	DP
2	UNB1 and UNB2	Constant force	Berthing and quayside
3	UNB1	PID	Unberthing and DP
	UNB2	Constant force	Unberthing
4	UNB2	PID	DP

4.2.1 DP

DP controlling is suitable for low-speed manoeuvring (Fossen 2011), hence switching from transit mode to DP mode is expedient when the vessel approaches the quay and the velocity is reduced. Due to the manoeuvring challenges that occur in the event of entering the quay it is convenient to switch from a 1 DOF transit controller to a 3 DOF DP controller. The DP controller is able to adjust the both heading and position towards the quay. The DP controller used in this thesis is a PID controller with feedforward action as described in Section 2.2.2.

The DP controller is again activated in the event of leaving the quay. To avoid windup of the integral term u_I in the PID controller while the berthing and unberthing controllers are activated, the integral term is frozen until the DP controller is enabled, as shown in (4.1)

$$u_I = \begin{cases} -K_i \int \tilde{\boldsymbol{\eta}} dt, & \text{with DP enabled} \\ 0, & \text{with DP unabled} \end{cases} \tag{4.1}$$

4.2.2 Berthing and Quayside

In the modes of berthing and quayside, the berthing controller is enabled. The berthing mode is when the vessel is berthing, starting at some predetermined short distance from the quay ending with the vessel at quayside. The berthing controller used in this thesis is a constant force pushing the vessel towards the quay, when the vessel is at a predetermined desired distance to the quay $\tilde{\boldsymbol{\eta}}_b$. $\tilde{\boldsymbol{\eta}}_b$ is defined in (4.2) with $\boldsymbol{\eta}_q$ and $\boldsymbol{\eta}$ being the quay and vessel positions respectively.

$$\tilde{\boldsymbol{\eta}}_b = \boldsymbol{\eta}_q - \boldsymbol{\eta} \tag{4.2}$$

The constant force is determined by freezing the value of $\boldsymbol{\tau}_{PID}$ at $\tilde{\boldsymbol{\eta}}_b$. In addition to the value from the DP controller, a bias force must be supplemented to ensure sufficient force in case of changes in weather. The final berthing controller is shown in (4.3).

$$\boldsymbol{\tau}_b = \boldsymbol{\tau}_{PID_{\tilde{\eta}_b}} + b \tag{4.3}$$

Where $\boldsymbol{\tau}_b$ is the commanded berthing thrust, $\boldsymbol{\tau}_{PID_{\tilde{\eta}_b}}$ is the commanded thrust from the PID controller in the event of initialisation of the berthing, and b is the bias. As the magnitude of $\boldsymbol{\tau}_{PID}$ is determined by the weather, so is $\boldsymbol{\tau}_{quay}$. The bias is a constant that should be determined based on the vessel type and quay environment. To avoid sudden changes of commanded force and to avoid unnecessary wear and tear of the actuators, the bias force is linearly increasing over some period of time until the maximum bias is reached displayed in (4.4).

$$b^N(t) = \begin{cases} b_{max}\frac{1}{T}t, & 0 \leq t < T \\ b_{max}, & t \geq T \end{cases} \tag{4.4}$$

Here $b^N(t)$ is the time dependent bias force in the NED frame, b_{max} is the maximum bias and T is some time constant. t is reset to $t = 0$ when the vessel is at quay. When $t \geq T$ the bias is a constant force in the NED frame $b^N = b_{max}$. As the goal is for the vessel to be pushed against the quayside, the bias force should be kept constant towards the quay in the NED frame. As forces are in the body-frame, a rotation dependent on the vessel angle ψ, and the quay angles β_1 and β_2 must be performed as shown in (4.5)-(4.6).

$$b_x^b = b^N(cos(\beta_1 - \psi) + cos(\beta_2 - \psi)) \tag{4.5}$$

$$b_y^b = b^N(sin(\beta_1 - \psi) + sin(\beta_2 - \psi)) \tag{4.6}$$

The superscripts N and b represent the NED and body-frame respectively, and x and y subscript symbolize the body-frame axis of the vessel.

The magnitude of the force exerted towards the quay during time of berthing and quayside, $\boldsymbol{\tau}_b$, should be big enough to withstand changes in weather while the vessel is docked. However, it is unnecessary to exert a huge force towards the quay in calm weather. The berthing force can be tuned depending of type of vessel and quay environment. For sheltered quays the berthing force can be smaller than for more exposed quays. In this thesis the bias in the berthing force is set to 10% of the maximum force of the vessel, after recommendation from Steinsvik (2019*b*) and Steinsvik (2019*a*).

The advantage of applying a constant berthing force, instead of using a PID controller for docking, is the ability to withstand sudden changes in the weather when docked, as the output of a PID controller decreases towards zero as the desired quay position is reached.

4.2.3 Unberthing

To be able to leave the quay without being slammed against it, an unberthing force is applied. The unberthing force can be implemented in several different ways, but it is critical that it is of sufficient magnitude. As previously mentioned, two different unberthing algorithms are developed and tested, referred to as unberthing method 1 or **UNB1**, and unberthing method 2 or **UNB2**. A description of the two unberthing methods follows.

Unberthing Method 1 (UNB1)

The first unberthing method is unberthing using the same controller as in the DP mode (4.7).

$$\boldsymbol{\tau}_{UNB1} = \boldsymbol{\tau}_{DP} \tag{4.7}$$

The advantage of using the same DP controller is a simpler controller structure and less tuning than with a specific controller for unberthing. However, the DP controller is dependent on the error between both the current position and velocity of the vessel, and the desired position and velocity generated by the reference model, $\tilde{\boldsymbol{\eta}}$ and $\tilde{\boldsymbol{\nu}}$. As the position and the desired position both are at the quayside when the unberthing phase is initiated, the DP controller has a slow response that may lead to slamming against the quay if the vessel is exerted to weather loads such as wind and waves.

Unberthing Method 2 (UNB2)

The second unberthing method uses a constant force for unberthing. The force is activated when the controller is switched between berthing and unberthing. Deactivation of the unberthing force happens when the vessel reaches a certain distance to the quay. The constant force is equal to the berthing force, but with opposite direction (4.8).

$$\boldsymbol{\tau}_{UNB2} = -\boldsymbol{\tau}_b \tag{4.8}$$

Compared to the first unberthing method, UNB1, this method is more complex as two different controllers are used when leaving the quay; unberthing and DP. The advantage of this method is the immediate response of the vessel's position when the unberthing controller is activated. However, as the reference model is not responding as fast as the vessel's position, an overshoot and oscillation occurs when the DP controller is activated.

4.3 Reset of the Reference Model

To be able to get a smooth and instantaneous response in the event of unberthing, it is expedient to reset the reference model. For UNB1, the desired outcome of resetting the reference model is to ensure an instantaneous movement of the vessel from the quay when unberthing is initiated. For UNB2 the goal of resetting the reference model is to avoid oscillatory behaviour.

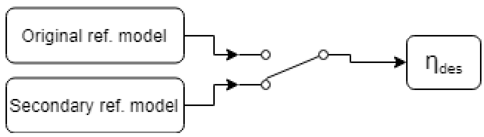

Figure 4.3: Switching between reference models. The enabled model creates the path for $\boldsymbol{\eta}_{des}$.

The method used to reset the reference model is to run two separate reference models, one with the desired position at the quay, and one with the desired position some distance from the quay. When the unberthing phase is entered a switch occurs between the two reference models as shown in Figure 4.3. In the berthing phase, the original reference model is enabled, with desired position at the quay. For the unberthing phase, a second reference model is used, hereafter referred to as the secondary reference model. The paths created by the two different reference models are displayed in Figure 4.4.

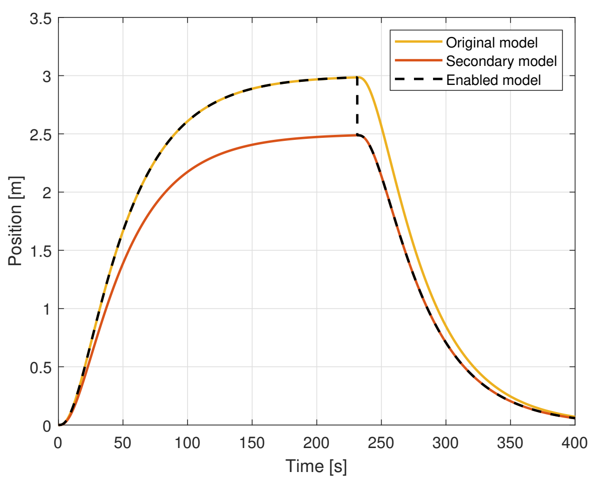

Figure 4.4: Reset of the reference model. Two separate paths are generated by two separat reference models. The original model generates a path from start point to quayside to endpoint, while the secondary model creates a path from start to some distance from the quay to endpoint. Switching between the models happens in the event of unberthing.

Setting the secondary reference model some distance from the quay causes a faster response for UNB1, as the PID controller instantly reacts to the error between the desired position and the present position. For UNB2, a switch in the reference model is necessary, as the unberthing force leads to an overshoot of the original reference model, causing oscillatory behaviour. The effects of resetting the reference model for both UNB1 and UNB2 is shown in Section 5.3.1.

The need for two separate reference models is a consequence of the type of reference model utilised in the simulation environment used in this thesis, MCSim. MCSim is described in Section 5.1.1 and the reference model is as the one described in Section 2.2.2. Due to the path generation being independent of the actual position of the vessel, it is impossible to change the path to start at a convenient position for the unberthing, hence the switching between reference models is necessary. Using another type of reference model where the path can be changed depending of the actual position of the vessel would be advantageous as there would be no need for creating two separate paths.

It is possible to achieve the desired outcome of resetting the reference model by letting the set-point of original reference model be outside of the quay. However, placing the set-point outside of the quay from the start leads to a slower response in the berthing phase, hence it is convenient to switch between two separate reference models.

4.4 The Supervisor and Switching Logic

The supervisor switches between the different controllers for the different stages ensuring the right controller to be enabled at each instant of time. Figure 4.5 shows the switching logic for the supervisor. $sup = 1, 2, ...4$ is the supervisor signal, corresponding to a specific controller. As the berthing/unberthing process is in focus for the development of this algorithm, the system starts in DP mode with $sup = 1$.

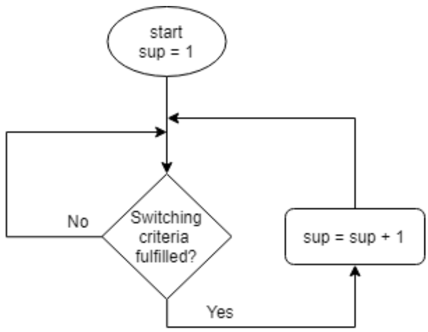

Figure 4.5: Switching logic for the supervisor. sup is the supervisor signal corresponding to the controllers. The switching criteria is different for each use mode.

The switching happens linearly, from controller 1 to 2, 2 to 3 and so on. The linearly switching is assured by a criterion of not switching to controller 2 unless controller 1 is enabled, and likewise for the rest of the controllers. The linear switching criteria is displayed as $sup = sup + 1$ in Figure 4.5.

The switching criteria is different for each switch and the switching can be initialised either when a specific position is reached, or a predetermined period of time has passed. For the first switch, from the DP controller to the berthing controller, a defined position must be reached for the switch to be carried out. When the vessel is sufficiently close to the quay in both x- and y- directions, the supervisor switches to the berthing control. The berthing control is enabled until the next stage of the process is entered; unberthing.

The switching from berthing to unberthing can be initialised by several factors. It can be convenient that a responsible person, for example the captain or mate, signals when the unberthing process should start. In the case of a ferry transporting cars back and forth over a fjord, a vision-based signal can be used to be able to determine when the cars queuing on the quay are all boarded. For simplicity the switching between berthing and unberthing is made time dependent in this thesis.

For the unberthing stage, the supervisor is dependent on which unberthing method is used. For the direct DP method (UNB1), the supervisor switches directly to the DP controller when the unberthing process is initiated. For the constant force method (UNB2), the supervisor switches from the berthing controller to an unberthing controller. The unberthing controller is then enabled until a certain position is reached, and the final switch is exerted from the unberthing controller to the DP controller.

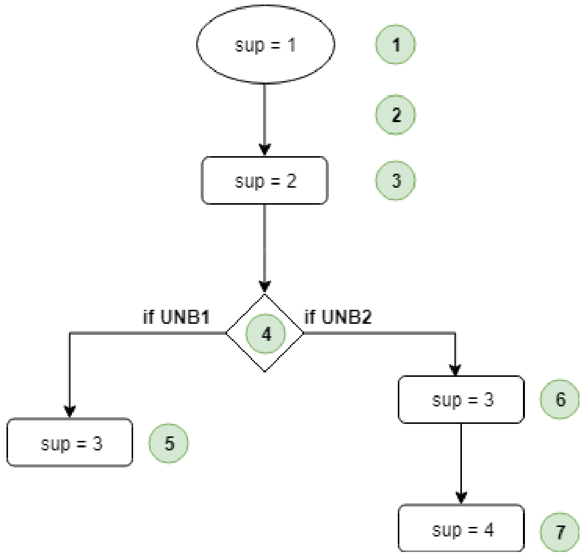

Figure 4.6: Flowchart showing the switching logic throughout the berthing/unberthing process.

A flowchart of the switching is shown in Figure 4.6, and each step is described below.

1. The docking is initialised and the DP controller is enabled.
2. The vessel is moving towards the quay.
3. The desired position of berthing is reached and the berthing controller is enabled. Berthing time is recorded.
4. Desired time at quayside is reached, unberthing phase is initialised.
5. UNB1: DP controller is enabled, vessel is unberthing.
6. UNB2: Unberthing controller is enabled, vessel is unberthing.
7. UNB2: Desired position of unberthing is reached, DP controller is enabled.

4.4.1 Switching from Unberthing to DP with UNB2

A problem concerning the switching between the unberthing controller and the DP controller when UNB2 is utilised (from 6 to 7 in Figure 4.6), is the fact that the vessel may not reach the desired position for switching in x- and y-directions simultaneously. This problem occurs mainly when there are some weather loads acting on the vessel, causing different loads in the x- and y-directions.

The switching from unberthing to DP control can be enabled with different switching criteria. Two different criteria for switching are discussed here, hereafter referred to as switching criteria 1, **SW1**, and switching criteria 2, **SW2**.

Switching Criteria 1 (SW1)

The first switching criteria is to switch when a certain position $\boldsymbol{\eta}_{sw}$ is reached in either x- or y-direction:

$$sup = 4 \quad \text{if} \quad \boldsymbol{\eta}_X >= \boldsymbol{\eta}_{sw_X} \quad \text{OR} \quad \boldsymbol{\eta}_Y >= \boldsymbol{\eta}_{sw_Y}$$

A disadvantage With this switching criteria is that since the switching position $\boldsymbol{\eta}_{sw}$ only needs to be reached in *one* of the directions, the position in the direction of which$\boldsymbol{\eta}_{sw}$ is not reached will be behind the reference model when switching to the DP controller. This is due to the set-point of the secondary reference model being placed at the switching position for both x- and y-direction. Hence, using the first switching criteria may lead to a rough path.

Switching Criteria 2 (SW2)

The second switching criteria is to switch to DP when a certain position $\boldsymbol{\eta}_{sw}$ is reached for both x- and y- directions:

$$sup = 4 \quad \text{if} \quad \boldsymbol{\eta}_X >= \boldsymbol{\eta}_{sw_X} \quad \text{AND} \quad \boldsymbol{\eta}_Y >= \boldsymbol{\eta}_{sw_Y}$$

With this switching criteria the unberthing force is exerted in both directions until the position of switching is exceeded in both directions. A disadvantage with SW2 is that when the vessel is unberthing faster in one direction than in the other, due to for instance weather loads, huge overshoots are to be expected in the direction of which the vessel moves faster.

4.5 Weather Dependency

For UNB1 the DP controller quickly responds to the weather changes, thus there is no need for implementing an algorithm to account for changes in the weather. However, the system is somewhat sensitive to weather changes if the secondary reference model is placed close to the quay. In extreme weather or in situations where the quay is exposed to sudden weather changes of great magnitude, it should be considered to either implement a weather-dependent unberthing force or set the secondary reference model to be further from the quay.

With UNB2, the weather has great impact on the response of the vessel during unberthing as a result of the unberthing force being constant. The magnitude of the unberthing force in UNB2 is the same as the berthing force, as described in Section 4.2.3. The magnitude of the berthing force, and thus the unberthing force, is decided and dependent on the weather at berthing as described in Section 4.2.2. The consequence of this algorithm is the ability of unberthing in the same weather, however, a drastic change in weather when the vessel is quayside may lead to either the vessel ejecting out from quay and overshooting the reference model, or being unable to unberth - depending on the angle and magnitude of the weather change. In worst case, the vessel can end up slamming against the quay, causing great damage.

To prevent possible damages of the ship when unberthing using UNB2 in alternating weather, the difference of magnitude in weather is implemented in the unberthing force algorithm as shown in (4.9)

$$\boldsymbol{\tau}_{UNB2} = -\boldsymbol{\tau}_b + \tilde{\boldsymbol{\tau}}_w \tag{4.9}$$

where $\boldsymbol{\tau}_b$ is the berthing force and $\tilde{\boldsymbol{\tau}}_w$ displays the change in weather forces from berthing to unberthing as shown in (4.10), where $\boldsymbol{\tau}_{w_b}$ is the weather loads at berthing and $\boldsymbol{\tau}_{w_{unb}}$ is the weather loads at unberthing.

$$\tilde{\boldsymbol{\tau}}_w = \boldsymbol{\tau}_{w_{unb}} - \boldsymbol{\tau}_{w_b} \tag{4.10}$$

Implementing a weather-dependent unberthing force leads to the unberthing force being less with wind from land and greater with wind from sea.

Chapter 5

Case-Study

The purpose of the case-study is to show by simulation the performance of the docking algorithm developed in this thesis. The following sections describe the simulation set-up, including the simulation environment where the case-study is performed, the vessel used and some tuning and simplifications. Further the simulation scenarios are presented before the simulation results are displayed and discussed.

5.1 Simulation Set-Up

5.1.1 Simulation Environment (MCSim)

The simulation environment used for development and testing of the docking algorithm is called MCSim (Marine Cybernetics Simulator) and is a Simulink model, including simulation models of a supply ship and a model vessel called Cybership 3. MCSim was initiated by A. J. Sørensen and developed by Ø. N. Smogeli and MSc students in the early 2000s (Perez et al. 2006). The toolbox has been further developed over several years by various professors, PhD candidates and MSc students at the Institute of Marine Technology at NTNU. The purpose of MCSim is to be an educational resource in fields of hydrodynamics, structural mechanics, machinery systems, and marine control and navigation systems (Sørensen et al. 2003). For instance, it is beneficial for master students to be able to develop and test different control systems, or parts of control systems, without having to build a simulation model from scratch.

MCSim consists of an environment module and a vessel module. The environment module calculates the different loads from wind, wave, current and ice and proceeds to feed them to the vessel module. The vessel module originally consists of vessel dynamics, sensor module, vessel controller and thruster module. In addition, a quay force module has been added to include the effects of the quay in the docking operation. For details concerning the design philosophy of MCSim see Sørensen et al. (2003), however multiple alterations have been conducted in the later years. Figure 5.1 shows the layout of the vessel module in Simulink. The following sections involve a brief description of the vessel module, consisting of both the original components and the segments added during the work of this thesis. Appendix A contains some description of what the different Simulink modules and MATLAB files contain.

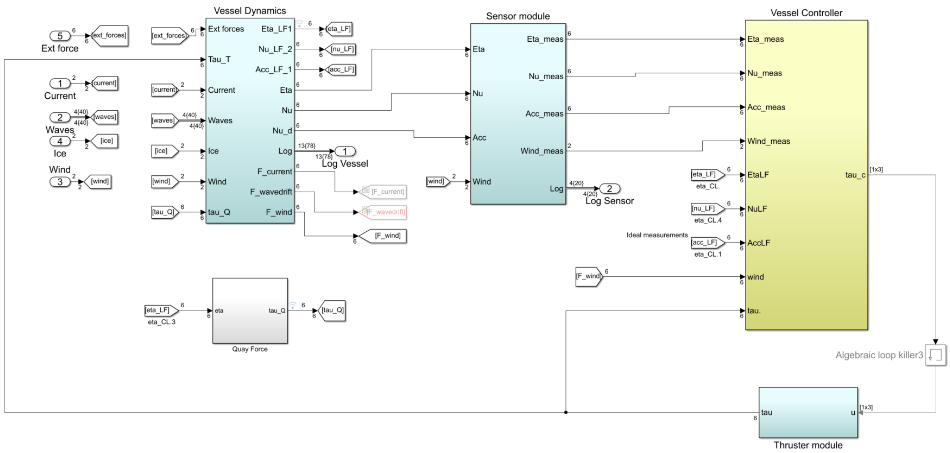

Figure 5.1: Schematic display of the vessel module. Print screen from MCSim.

Quay Module

The quay module is added to MCSim to be able to simulate forces working on the vessel from the quay when the vessel is quayside. The inputs of the quay module are the 3 DOF vessel positions, and the outputs are the 6 DOF quay forces, τ_q, where the forces in x- and y-directions are the only non-zero elements. The quay forces are as described in Section 2.1.4.

Vessel Dynamics

The vessel dynamics consist of a 6DOF LF model and a 6DOF WF model (see section 2.1.3). The inputs are the loads from the environmental module, loads from the quay when the vessel is at quayside, and thruster loads. The outputs are the positions $\boldsymbol{\eta}$ in NED frame, the velocities $\boldsymbol{\nu}$ and the accelerations of the vessel in body-fixed frame.

Sensor Module

In the sensor module, noise is added to the actual position, velocity and acceleration of the vessel in addition to the wind load from the environmental module. This to create somewhat realistic values from the sensors, as sensor noise is inevitable.

Vessel Controller

The vessel controller block consists of a reference model, an observer, and a controller module. The inputs are the measurements of the wind load, vessel position $\boldsymbol{\eta}$ in NED, vessel velocity $\boldsymbol{\nu}$ and acceleration in body-fixed frame, in addition to the ideal measurements and the thruster force τ. The output is the controller force τ_c. The reference model is similar to the one described in Section 2.2.2, the observer is a non-linear passive observer and the original controller is a PID controller included feedforward control. Both the controller module and the reference model module are adjusted for the system to be able to perform as desired. The observer is kept unaltered.

In the controller module, a berthing controller, an unberthing controller, a supervisor and a switch is implemented to be able to perform autonomous docking. The berthing and unberthing controllers are implemented as described in sections 4.2.2 and 4.2.3 respectively. The supervisor and switching logic is described in Section 4.4. The final block-diagram of the controller system is shown in Figure A.2 in Appendix **??**.

A secondary reference model is added to the reference module, to be able to operate with an original and secondary reference module as explained in Section 4.3. The secondary reference model is identical to the original one, with the only difference being the set-point of the desired position.

Thruster Module

The input of the thruster module is the commanded force from the vessel controller, τ_c, and the output is the thruster force τ. There is no thrust allocation, thus there is no distribution of the commanded force to the thrusters, and only the total thrust for the vessel is considered. The forces in surge, sway and yaw are saturated by the total maximum thruster force. The maximum force for Cybership 3 is set to be $\tau_{max} = [10, 10, 12]^T$ N.

In addition to the force saturation, a rate limit is included in the thruster module to prevent the thruster force to be changed instantaneously. The rate limiter is designed as a first order transfer function (5.2), derived from the differential equation (5.1) with time constant $T = 0.5$ for surge, sway and yaw for Cybership 3. u and y is here the thruster force before and after the rate limiting respectively.

$$T\dot{y}(t) + y(t) = u(t) \tag{5.1}$$

$$G(s) = \frac{Y(s)}{U(s)} = \frac{1}{Ts + 1} \tag{5.2}$$

5.1.2 Vessel Characteristics for Cybership 3

Figure 5.2: Cybership 3 (Brodtkorb 2017).

The vessel used in this case-study is a model ship named Cybership 3 (CS3) from the Marine Cybernetics Laboratory (MCLab) at Institute of Marine Technology at NTNU in Trondheim. Figure 5.2 shows the model ship CS3, which is a model of a platform supply vessel (PSV), in a scale of 1:30. The vessel was built by Sintef Ocean (former Marintek) in 1988. The principle hull data for the model- and full-scaled PSV is listed in Table B.1 in Appendix B. The hull has remained the same, but the mass distribution has been changed as the equipment has been alternated. The structure mass distribution was calculated with the current equipment in 2015. Both the original and revised structure mass distribution is presented in Table B.2 in Appendix B. For a more extensive description of Cybership 3 see Appendix B.1 in Brodtkorb (2017).

5.1.3 Tuning

Figures 4.1 and 5.3 shows the different modes of operation. The switching between the corresponding controllers for these modes must be tuned for the docking algorithm to perform optimally. In addition, the resetting of the reference model must be tuned. The different parameters are dependent of the weather, placement of the quay and type of vessel. The two different unberthing methods discussed in this thesis needs to be separately evaluated for tuning considering parameters involving the unberthing. The tuning and initialisation parameters are listed in Table 5.1 and described in the following sections.

Table 5.1: Tuning and initialisation parameters

Tuning parameter	Value	
Berthing initialisation	-0.5 m	rel. to the quay
Unberthing initialisation	100 s	from berthing initialisation
DP initialisation for UNB2	-0.5 m	rel. to the quay
Reset of ref. model (UNB1)	-0.5 m and -0.1 m	rel. to the quay
Reset of ref. model (UNB2)	-0.5 m	rel. to the quay

Initiating the Berthing Controller

The initiation of the berthing controller is dependent on the position of the vessel relative to the quay position. The distance to the quay where the switching occurs can be tuned to get an earlier or later switch. The earlier the switch is made, the sooner the vessel will be docked. However, a too early switch to the berthing control may lead to instability, or the vessel may collide into the quay with a huge force as the berthing force is constant. A late switch may on the other hand cause the vessel to be out of control and vulnerable to the weather forces, as the force from the DP controller is decreasing towards zero as the position error is reduced. The chosen position of berthing is at 0.5 m from the quay, in both x- and y-directions.

When unberthing with UNB1, the time of initiation of the berthing controller is of no significance, but with UNB2, the embarkation of the berthing controller is affecting the magnitude of the unberthing force, and hence it is of importance. The berthing force is calculated to be the DP force at the time instant where the switching between the DP controller and the berthing controller occurs in addition to a bias, and as the DP value is decreasing towards 0, the berthing force is dependent of the time of switching. A late switch will give less magnitude than an early switch. As the unberthing force is determined to be of same magnitude as the berthing force, the unberthing force is dependent on the time of switching from DP to berthing control.

Switching to DP for UNB2

The switch between the unberthing controller in UNB2 and the DP controller happens when the vessel reaches a desired distance from the quay. It is desirable that the switching from unberthing controller to DP controller happens when the vessel is far enough from the quay to avoid slamming against it. When the unberthing controller is enabled, the vessel is not controlled as it is only pushed away from the quay with some force. Thus, it is expedient to switch to the DP controller as soon as possible to obtain a desired position and finally being able to transit. The switching between unberthing controller in UNB2 and the DP controller is in this thesis initiated when the vessel is 0.5 meters from quay in either x- or y-direction for SW1 and in both x- and y-directions for SW2.

Resetting of the Reference Model

The resetting of the reference model is described in Section 4.3. How far from the quay the set-point for the secondary reference model is placed can be tuned in order to get a smooth departure for the vessel.

For UNB1, a set-point far from the quay will give an immense unberthing force and may lead to an overshoot and oscillations. On the other hand, placing the secondary set-point too close to the quay may lead to the vessel being unable to leave the quay smoothly in extreme weather. Hence, the placement of the secondary set-point should be tuned in order to generate a smooth path out from quay. In this thesis, resetting the reference model to both 0.5 and 0.1 meters are tested to evaluate the advantages and disadvantages of placing the set-point for the secondary reference model to be relative close and relative far from the quay.

For UNB2, the placement of the secondary set-point should be placed such that the position of the vessel and the desired position from the reference model is approximately the same at the time of switching between the unberthing controller and the DP controller. The reason for this is to avoid overshooting if the vessel position is behind the reference model, and to avoid oscillations and reversing if the vessel position is in front of the reference model. This is achieved by setting the secondary set-point to the position of which when reached, the switching between the unberthing controller and the DP controller is initiated - at 0.5 meters from the quay.

5.1.4 Simplifications

Some simplifications are made in order to be able to perform the simulations in a feasible way. The simplifications are listed below.

- The vessel is considered as a single point (CoG) when it comes to the position measurements. The distance from the vessel's current position to the quay is derived from the position measurements, leading to a peculiar case. When the vessel is at quay it is the CoG that is at quayside, thus the vessel is half its breadth beyond the quay. As this thesis only considers simulations, this has no impact here. However, if the algorithm were to be tested in a laboratory experiment this issue should be dealt with.

- Quay forces works only perpendicular to the quay; hence the vessel is able to slide against the quay with no friction. Additionally, the forces from the quay are working throughout the whole quay axes. In the simulations these simplifications have no impact as long as the vessel is able to unberth and leave the quay as intended. However, in situations where the vessel is unable to unberth some unrealistic behaviour is expected.

- The quay has no impact on the wind. Meaning that with wind from land, the wind loads acts on the whole vessel, while in fact some of the vessel is covered by the quay. The cover the vessel experience from the quay is dependent on the quay, the tide and the vessel. In some cases, the vessel may even be fully covered by the quay and the wind loads have no impact on the vessel until it is some distance from the quay. In this case-study, the quay is considered as a one dimensional line, hence the wind load is working on the whole outer area of the vessel.

- Only wind is considered in the simulations. The other weather forces, current and wave loads are neglected. In a docking scenario, both wave and current loads often are small due to the sheltered environment surrounding the quay. However, in extreme weather current loads and especially wave loads have great impact on the vessel and may cause trouble if not considered.

- There is no thrust allocation in the thruster module, so the thrust force is applied from one single point on the vessel (CoG). Further, only the total maximum force is limited, not the specific maximum force for the different thrusters. With no thrust allocation, the simulations become somewhat unrealistic as challenges considering the different thrusters' placement, force limitations, rotation possibility and the interaction between the thrusters are neglected.

- The wind neutralising algorithm for UNB2 discussed in Section 4.5 considers the wind forces working on the vessel, calculated in the vessel dynamics module. Thus, the actual wind loads are implemented in the algorithm. This is a simplification, as the wind sensors will never be able to give such accurate output.

5.2 Simulation Scenarios

The simulation scenarios are constructed to show how the unberthing algorithm works and how some parts of the algorithm are essential in various situations. Figure 5.3 shows a visualisation of the docking process simulated in this case-study. Here, the simulation starts with the vessel being in the origin of the local NED frame $\boldsymbol{\eta}_{init} = [0, 0, 0]^T$, with zero velocity. The quay is positioned at $\boldsymbol{\eta}_q = [x_q, y_q, \psi_q]^T = [3, 5, \pi/2]^T$. When the quay is reached, the vessel is at quayside for 100 seconds before the unberthing is initialised. The final vessel position is at the origin of the same local NED frame, but with the vessel rotated 180 degrees $\boldsymbol{\eta}_{end} = [0, 0, \pi]^T$. As the simulations are performed using the vessel characteristics of a model ship, the distances and the wind loads are small compared to appropriate values for a full-size vessel.

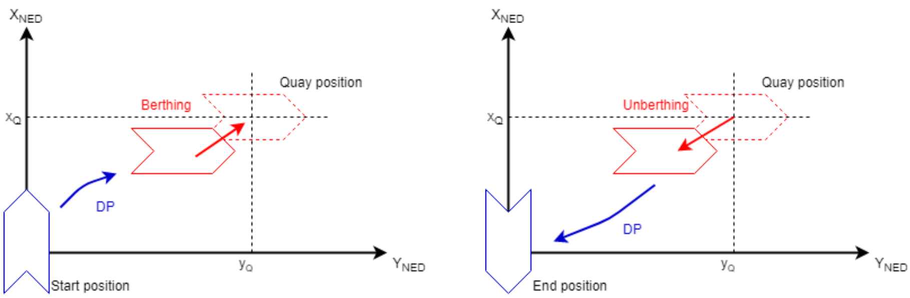

(a) Vessel starting in the origin, ending at the quay position.

(b) Unberthing of the vessel and ending at the end position at the origin.

Figure 5.3: Visualisation of the docking process.

In the first scenario, presented in Section 5.3.1, the differences of unberthing with and without resetting of the reference model for both UNB1 and UNB2 are presented and discussed. There is no weather acting on the vessel in the first scenario. For UNB1 the difference of resetting the reference model to 0.1 m and 0.5 m are shown.

The second scenario, presented in Section 5.3.2, shows the unberthing of the vessel with UNB1 and UNB2 when wind loads are applied. For UNB1 the responses of resetting the reference model for different set-points for the secondary reference model is once again compared. For UNB2 the responses with and without wind feedforward control implemented is shown, in addition to a comparison of using different switching criteria when switching from the unberthing controller to the DP controller, SW1 and SW2. The scenarios are listed in Table 5.2 below.

The wind applied in the second scenario is activated after 180 seconds, while the vessel is quayside. Hence, the wind load is different from berthing to unberthing. The wind applied is from south $\psi_{wind} = 180°$, with 1 hour mean wind velocity at 10 meters of $U_{10} = 2.7 m/s$. As the wind is applied when the vessel is at quay and positioned with an

Table 5.2: Description of the different simulation scenarios

Scenario 1	Effect of resetting the reference model
Scenario 2	Responses of weather changes during docking

angle $\psi = \pi/2$, the wind load is mainly acting towards the starboard side of the vessel, pushing it towards the quay. It is therefore expected for the vessel to struggle to unberth in the NED x-direction.

The wind spectrum used for the simulation of the wind is the NORSOK spectrum. The magnitude of the wind velocity is the greatest possible without the vessel starting to move from quay before unberthing, determined by trial and error. Figure 5.4 shows how the wind loads in the vessel's body-frame varies with the angle of the vessel ψ. The maximum magnitude of the wind loads is below 1 N in the y-direction, and just above 1 N in the x-direction. Gust is not implemented, neither is variation of the wind direction.

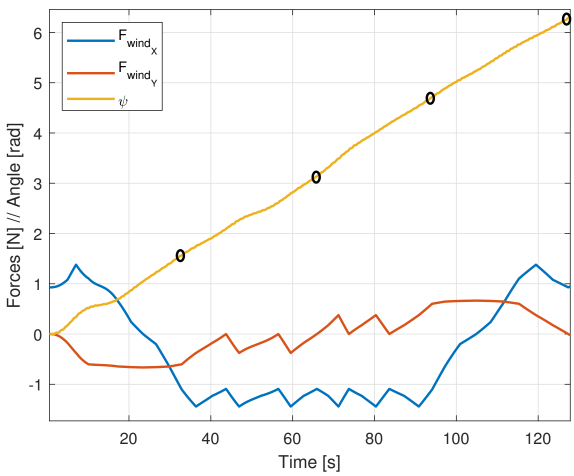

Figure 5.4: Wind loads in x^b- and y^b-directions with varying ψ. The circles display the angles of $\pi/2$, π, $3\pi/2$ and 2π.

5.3 Simulation Results

The results from the case-study are presented in this section. The plots presented are time plots of the positions and time plots of forces. The positions are in the NED frame, where η_X and η_Y are the measured positions in x- and y-directions, and η_{X_d} and η_{Y_d} are the desired positions generated from the reference model. The thrust and wind loads are in the body-fixed frame, where τ_c is the commanded thrust force, τ_{pid} is the thrust calculated in the DP controller and F_{wind} is the wind load. In every plot the signal from the supervisor is included to show which controller is enabled at each instant of time.

5.3.1 Scenario 1: Reset of the Reference Model

For the first scenario, a comparison of the unberthing with and without resetting the reference model is presented. In this scenario, no weather is acting on the vessel. The results are presented for UNB1 and UNB2 separately.

UNB1

Figure 5.5 shows the position response of unberthing with UNB1. From the figure, looking at the switching between controller 2 and 3, we see that the response is slow, and the vessel is at quayside for some time after the switch has been performed. The slow response is a consequence of the DP controller acting on the error between the current position and the desired position generated by the reference model, which at the event of switching is zero.

At the point of switching from controller 2 to 3 the berthing control is not active. Thus, there is no force holding the vessel against the quay, leading to a possible unwanted slamming against the quay in cases where waves and current loads are applied.

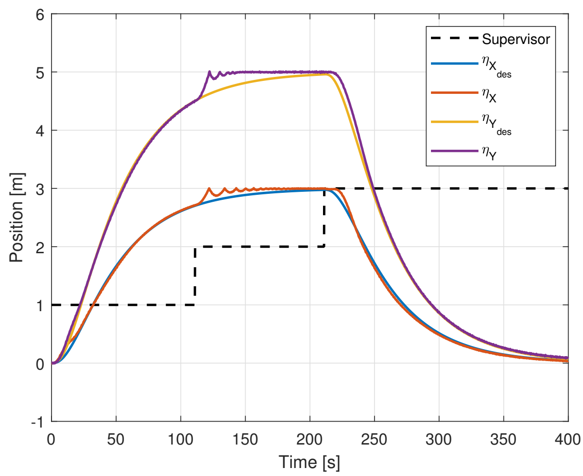

Figure 5.5: Scenario 1, UNB1: Position plot of the docking process. Unberthing without resetting the reference model.

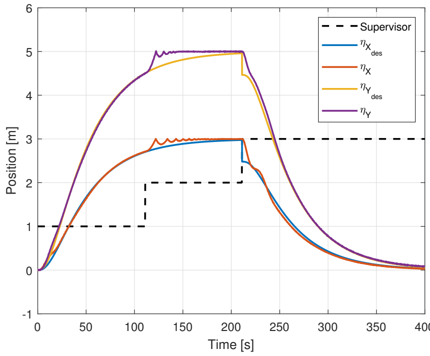

(a) Unberthing set-point at 0.5 m from quay.

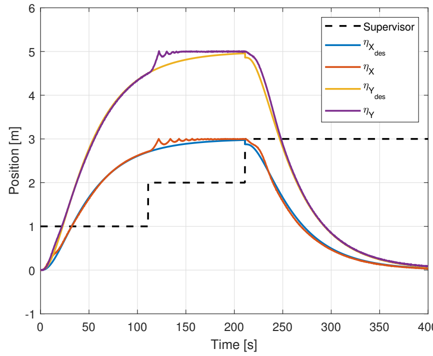

(b) Unberthing set-point at 0.1 m from quay.

Figure 5.6: Scenario 1, UNB1: Position plot of the docking process. Resetting the reference model with different unberthing set-points.

Figure 5.6 shows the response of resetting the reference model in the event of unberthing. The set-point of the secondary reference model is placed to be 0.5 meter from the quay in Figure 5.6a and 0.1 meter from the quay in Figure 5.6b. With a set-point further from the quay (5.6a), the unberthing force is greater than with a set-point close to the quay (5.6b). With a bigger unberthing force, the vessel is unberthing rapidly, but expires a small oscillation in $\boldsymbol{\eta}_x$. Using an unberthing set-point of 0.1 m from the quay, the unberthing happens slower but in a smoother manner. Comparing Figures 5.6a and 5.6b with Figure 5.5, the effect of resetting the reference model is clear as the unberthing happens immediately after initiated. The result of resetting the reference model is a solid foundation to be able to prevent clashes with the quay.

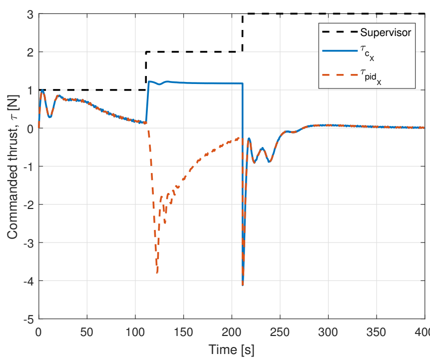

(a) Unberthing set-point 0.5 m from quay.

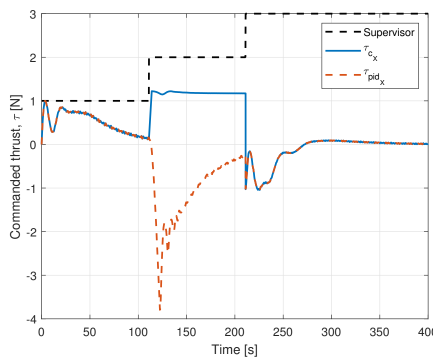

(b) Unberthing set-point 0.1 m from quay.

Figure 5.7: Scenario 1, UNB1: Commanded thruster force for the docking process. Resetting the reference model with different unberthing set-points.

Figures 5.7a and 5.7b show the commanded thruster force in x-direction for UNB1 with resetting the reference model to 0.5 m and 0.1 m from the quay respectively. For controller 1, the commanded force τ_{c_X} is equal to the DP force τ_{PID_X}. Upon switching to the berthing controller, τ_{c_X} is increased to a constant force as described in Section 4.2.2. The enabling of the berthing controller causes the position of the vessel to exceed the desired path as can be seen in Figures 5.5 and 5.6, causing τ_{PID_X} to expand in a negative matter. With the vessel steady at quayside and the path of the reference model approaching the position of the vessel, the magnitude of τ_{PID_X} is decreasing towards zero.

In the event of unberthing, the commanded force is again equal to the DP force $\tau_{c_X} = \tau_{PID_X}$. The reset of the reference model occurs in the switching between controller 2 and 3, and the difference of resetting the reference model to 0.5 m and 0.1 m is clearly shown comparing Figures 5.7a and 5.7b. Resetting the reference model to 0.5 meters from the quay creates an unberthing force of $\tau_{c_X} = -4N$, while resetting to 0.1 meters from the quay creates a lesser unberthing force, $\tau_{c_X} = -1N$.

UNB2

As there is no weather loads applied in this scenario, the different switching criteria discussed in Section 4.4.1 gives the same response, as the position for switching from unberthing to DP is reached simultaneously in x- and y-directions. Thus, only one of the methods are considered here.

Figures 5.8a and 5.8b show the position responses of unberthing without and with resetting of the reference model for UNB2 respectively. Unberthing with UNB2 without resetting the reference model leads to an oscillating behaviour of the position, caused by the desired position being exceeded when the unberthing controller is activated. Resetting the reference model in the unberthing phase leads to a smoother unberthing, as the desired position now is further from the quay and the switching to the DP controller occurs before the desired position is exceeded.

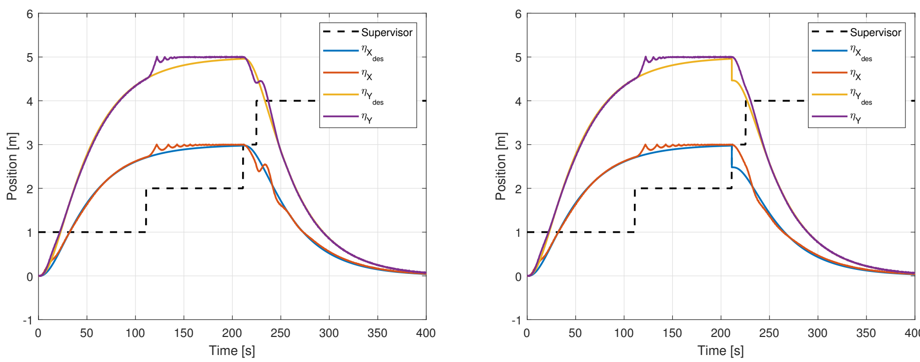

(a) Constant reference model.

(b) Resetting of the reference model implemented.

Figure 5.8: Scenario 1, UNB2: Position plot of the docking process. Effect of resetting the reference model in the event of unberthing.

Figure 5.9 shows the commanded thrust τ_{c_X} and the DP force τ_{PID_X} in x-direction, for unberthing with UNB2. In Figure 5.9a, the reference model is kept constant. The overshoot of the desired path in the event of unberthing causes τ_{PID_X} to increase rapidly to about $\tau_{PID_X} \approx 2.5N$ and then decrease to $\tau_{PID_X} \approx -1.5N$ before stabilizing.

In Figure 5.9b, the reference model is switched to a set-point 0.5 meters from the quay. Here the difference between force from the unberthing controller and the DP force is small, compared to Figure 5.9a. Hence, there is no sudden changes in the force magnitude.

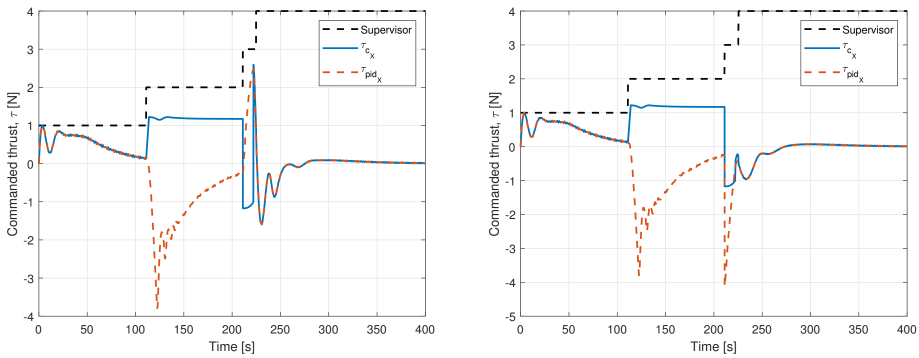

(a) Constant reference model.

(b) Resetting of the reference model implemented.

Figure 5.9: Scenario 1, UNB2: Commanded thruster force for the docking process. Effect of resetting the reference model in the event of unberthing.

5.3.2 Scenario 2: Effects of Wind

In the second simulation scenario wind is applied from south, pushing the vessel towards the quay in the x-direction in NED and in negative y-direction in the body-frame. A comparison of different set-point for the secondary reference model is presented for UNB1. For UNB2, the responses of unberthing with and without wind feedforward control is shown, in addition to comparing the outcome of using different switching criteria, SW1 and SW2.

UNB1

Figure 5.10 shows the response of unberthing with UNB1 with different placements of the secondary reference model. As the wind is coming from south and pushing towards the starboard side of the vessel, it is expected for the vessel to struggle unberthing in x-direction. Figures 5.10a and 5.10b show the unberthing with the secondary set-point at 0.5 and 0.1 meters from the quay respectively. In 5.10a, the vessel is able to withstand the wind, and the unberthing happens rapidly. In 5.10b the unberthing is slower and the vessel is at quayside in x-direction for some time after the unberthing is initialised. The extra unberthing force obtained by placing the set-point of the secondary reference model some distance from the quay is indeed needed in this case.

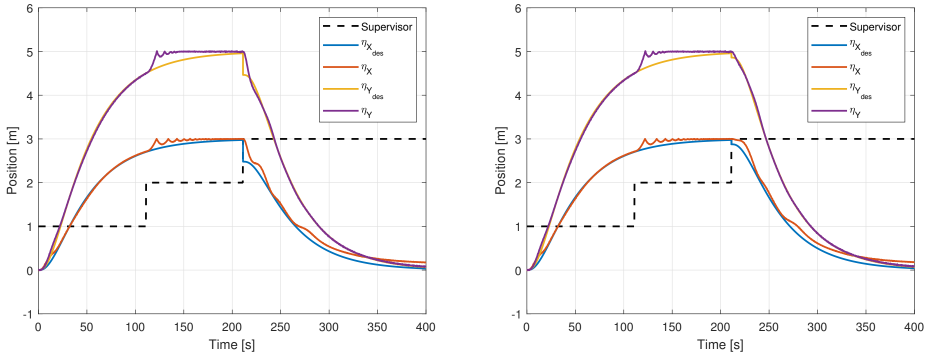

(a) Unberthing set-point at 0.5 m from quay. **(b)** Unberthing set-point at 0.1 m from quay.

Figure 5.10: Scenario 2, UNB1: Position plot of the docking process. Resetting the reference model with different unberthing set-points with wind loads acting on the vessel.

UNB2

Figure 5.11 shows the response of unberthing in wind with UNB2 using the first switching method, SW1, as described in Section 4.4.1. The response without and with the implementation of wind feedforward from Section 4.5 is shown in Figures 5.11a and 5.11b respectively.

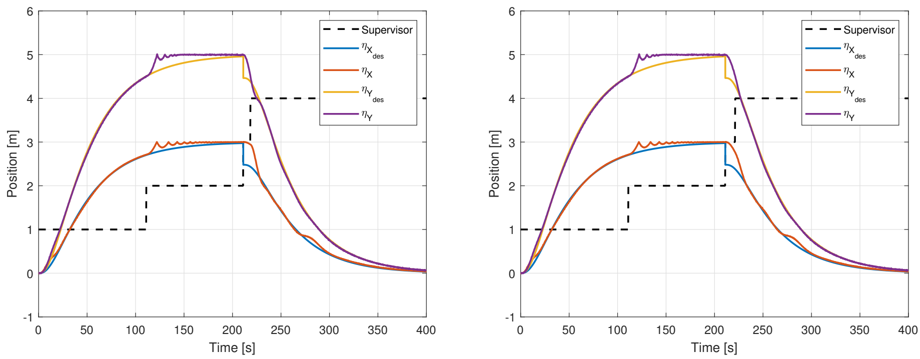

(a) Unberthing without wind feedforward. **(b)** Unberthing with wind feedforward.

Figure 5.11: Scenario2, UNB2: Position plot of the docking process. Comparing the unberthing using SW1 without and with the wind feedforward algorithm implemented.

From Figure 5.11a one can see that the unberthing happens in the x-direction than in the y-direction. This is due to lack of unberthing force. However, as the switching from unberthing to DP occurs when the desired position is reached in *one* of the directions, the DP controller is enabled after approximately 20 seconds. The switching to the DP controller gives enough force for the vessel to be able to unberth in x-direction aswell. Figure 5.11b shows that with the wind feedforward algorithm implemented, the unberthing happens more rapidly and the vessel is able to unberth in both directions before the switching to the DP controller takes place.

Figures 5.12 and 5.13 displays the position responses for unberthing with UNB2 and SW2, with a desired vessel angle of $\psi = \pi$ and $\psi = \pi/2$ respectively. Figure 5.12a shows that the vessel is unable to unberth in the x-direction, while the y-direction experience a quick response. The result is the vessel being dragged against the quay. This is a consequence of having an equal unberthing force in x- and y-directions, while the wind is affecting the vessel in x-direction more than in y-direction. The simulation is terminated at 290 seconds due to singularities.

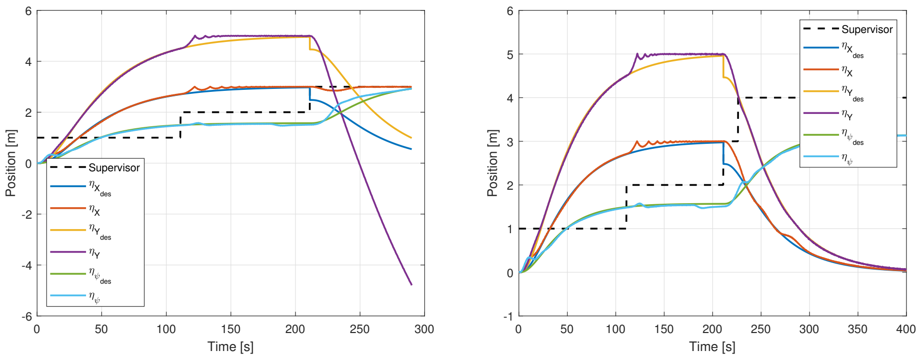

(a) Unberthing without wind feedforward. **(b)** Unberthing with wind feedforward.

Figure 5.12: Scenario2, UNB2: Position plot of the docking process. Comparing the unberthing using SW2 without and with the wind feedforward algorithm implemented. The final ψ_{des} is here π.

Figure 5.12b shows that with the implementation of the wind feedforward algorithm, the vessel is able to unberth in a smooth manner, and with the same result as with SW2 shown in Figure 5.11b. The reason for the similarity of SW1 and SW2 when the wind feedforward algorithm is implemented, is that the unberthing force is big enough in both x- and y- direction, causing the switching position of 0.5 meters to be reached simultaneously for η_X and η_Y, hence SW1 and SW2 provide the switching at the same time.

The vessel's ability to unberth with UNB2 and SW2 without wind feedforward is restored if the desired angle ψ_{des} is set to be constant at the unberthing $\psi_{des} = \pi/2$ instead of changing to $\psi_{des} = \pi$. Figure 5.13a shows the response of unberthing with UNB2 and SW2, $\psi_{des} = \pi/2$. The unberthing happens faster in the y-direction than in the x-direction as expected. Unlike with $\psi_{des} = \pi$, the vessel is able to leave the quay in x-direction. When the switching to the DP controller is initialised, the vessel has exceeded the desired path by approximately 1.5 m in y-direction. The overshooting leads to an unwanted bouncing back of the position in the y-direction. Figure 5.13b shows the response with the wind feedforward algorithm implemented and in the same manner as in Figures 5.11b and 5.12b, the unberthing happens smoothly.

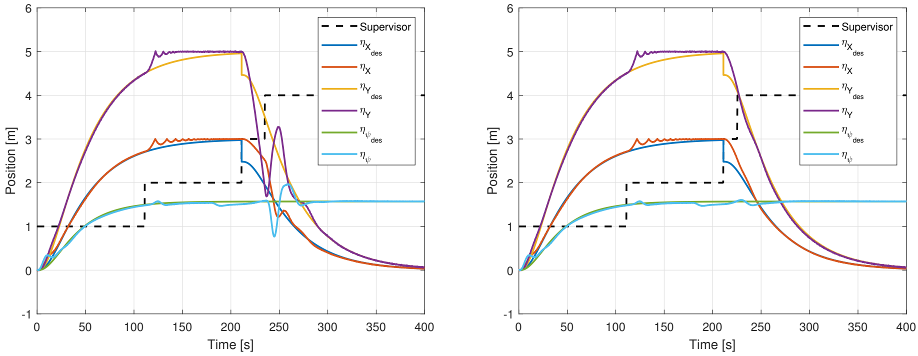

(a) Unberthing without wind feedforward. **(b)** Unberthing with wind feedforward.

Figure 5.13: Scenario2, UNB2: Position plot of the docking process. Comparing the unberthing using SW2 without and with the wind feedforward algorithm implemented. The final ψ_{des} is here $\pi/2$.

Figure 5.14 shows the command force τ_{c_x} and the wind load F_{wind_x} in the body-frame for unberthing with UNB2 and SW2 with $\psi_{des} = \pi$ in Figure 5.14a and $\psi_{des} = \pi/2$ in Figure 5.14b. Additionally, the vessel angle ψ and the supervisor signal is plotted. In Figure 5.14a the simulation is terminated due to singularities, while in Figure 5.14b the simulation was stopped right before the supervisor was switched to controller 4, to emphasize the unberthing phase.

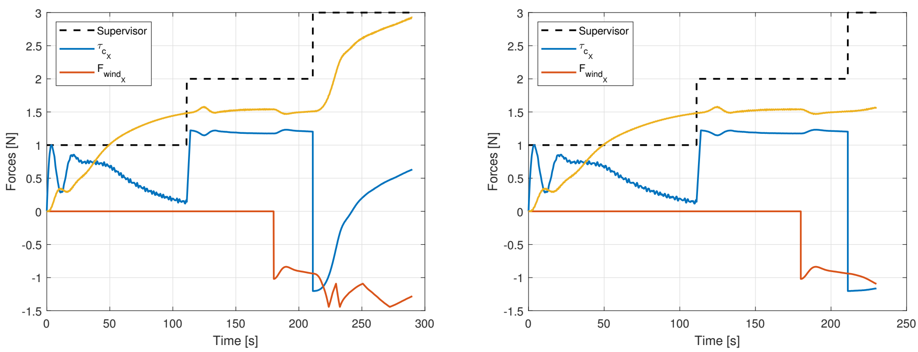

(a) Vessel turning from $\psi = \pi/2$ to $\psi = \psi$. **(b)** Vessel angle kept constant at $\psi = \pi/2$.

Figure 5.14: Scenario2, UNB2: Commanded thruster force and wind force in the vessel's x-direction. Comparing commanded thrust for when the vessel is turning at unberthing and when the vessel angle is kept constant throughout unberthing.

As the unberthing force is set to be perpendicular to the quay, the turning of the vessel from $\psi = \pi/2$ to $\psi = \pi$ leads to the unberthing force in the vessel's x-direction going from a negative to a positive force. The turning of the vessel does not affect the wind loads in the same manner, leading to the unberthing force in x to decrease, while the wind load in x is increasing. In this turning, the unberthing force in x is not big enough to unberth. In Figure 5.14a, $\tau_{c_x} > F_{wind_x}$ for a few seconds, resulting in the small response of the x-position in Figure 5.12a. When the angle of the vessel starts changing towards $\psi_{des} = \pi$, $\tau_{c_x} < F_{wind_x}$, and the vessel is pushed back towards the quay. Figure 5.14b shows that when the vessel angle is kept constant at $\psi = \pi/2$, $\tau_{c_x} > F_{wind_x}$, hence the vessel is able to unberth.

Chapter 6

Discussion

In this chapter the methods used for berthing and unberthing of the vessel are discussed in regards to simulation results, performance and possible improvements.

6.1 The Berthing Method

The aim of the berthing controller is for the vessel to dock to the quay and stay quayside for a given amount of time. In the docking algorithm developed during the work of this thesis, the berthing of the vessel is performed by applying a constant force towards the quay. The simulation results in Section 5.3 show that the berthing is performed with small clashes with the quay, occurring when the vessel reaches the quayside. As the vessel bounces less than 15 cm back, these clashes are considered to be small and acceptable. A smoother berthing can be achieved by switching from DP to berthing closer to the quay, leading to a slower berthing and less energy in the impact.

In the case-study, no weather loads are applied during the berthing. However, as the berthing force is equal to the force of the DP controller in the event of berthing, in addition to a bias, it is reasonable to assume that the berthing controller is able to perform desirable with weather loads as well. This assumption is based on the fact that the force commanded by the DP controller is dependent on the weather. When the bias force is added to the DP force, the total berthing force will be of sufficient magnitude for the system to perform as desired, even in rough weather.

Instead of switching to a berthing controller and applying a berthing force, the berthing can be performed by placing the set-point of the reference model some distance beyond the quay position. By doing so, the desired position will never be reached and the non-zero error causes the DP controller to create a force that will ensure berthing. With a constant error from the vessel's position at the quayside to the desired position beyond the quay, the proportional term in the PID controller creates a constant force ensuring the vessel to stay quayside. The integral term, on the other hand, will lead to an increasing force as the constant error is integrated over time. Hence, with the use of this method it is crucial to implement an anti-windup mechanism.

The performance of the system in the berthing phase can be as desired either the berthing is performed with a separate berthing controller as utilised in this thesis, or with a DP controller with set-point beyond the quay. This is as long as the berthing force is of suitable magnitude - decided by the bias and the set-point placement respectively. The advantage of using the DP controller for berthing is a less complex system without the berthing controller. The advantage of using a separate berthing controller, on the other hand, is the possibility of deciding the magnitude of the impact force with the quay and the force applied during quayside separately. This is decided by how far from the quay the switching from DP to berthing happens, and the magnitude of the bias respectively. By using a simple DP controller for berthing, both the speed of the vessel in the event of berthing and the magnitude of quayside force is dependent on the placement of the desired position. Thus, a need for alteration of the DP controller could be necessary in order to achieve desired performance regarding the berthing and quayside situation.

6.2 The Unberthing Methods

The performance of the two different unberthing methods presented in this thesis is shown in the simulation results of the case-study in Section 5.3. Both methods give a desirable outcome, as the vessel is able to unberth. However, both methods are dependent on the reference model being reset to perform optimally. Additionally, the wind feedforward control plays major role when unberthing with UNB2 in cases where wind loads are changed during time at quayside.

UNB1 has the simplest implementation; no additional controller for the unberthing is needed as the DP controller is used for unberthing. Nevertheless, some sort of unberthing force is needed to push the vessel rapidly from the quay to avoid the vessel slamming against the quay caused by e.g. wave loads when the berthing controller is deactivated. Resetting the reference model to some distance from the quay provides the unberthing force needed. Both 0.5 m and 0.1 m from the quay were investigated in calm weather and with wind loads activated. With zero wind loads, resetting the reference model to 0.1 m from the quay gave the best outcome. With wind loads acting towards the quay the force demand is higher and resetting the reference model to 0.5 m from the quay gave the best outcome.

With the type of reference model used in this thesis the resetting of the reference model is predetermined and the magnitude of the unberthing force for UNB1 is not dependent on the weather. This results in the same unberthing force being exerted in all kinds of weather. The outcome is an overshoot in calm weather or with wind loads directed from the quay, while with wind directed towards the quay the vessel may be unable to unberth before being slammed against the quay.

A solution to the issue addressed above is to use a reference model where the set-point can be changed during the operation. With such reference model the position of the set-point in the event of unberthing can be decided by the weather loads acting at unberthing. With weather directed from the quay the reference model should be set to be close to the quay, while with weather loads acting towards the quay the reference model should be set further from the quay to achieve the desired unberthing force.

UNB2 is a somewhat more complex unberthing algorithm than UNB1 with an extra controller for unberthing. The advantage of having an unberthing controller is the possibility to adjust the unberthing force to the weather, even with the predetermined reference model. A wind feedforward algorithm is added to the unberthing controller to ensure the unberthing force to be of sufficient magnitude.

The results from the case-study show that with the wind feedforward control implemented the vessel is able to unberth with no trouble and the vessel performance in calm and rough weather is identical. This result is as expected as the wind is simply cancelled out. The cancellation is a simplification as actual wind loads are considered here while in fact these loads are difficult to retrieve accurately. However, even with inaccurate wind measurements the algorithm will adjust the unberthing force to a more fitting magnitude unless the sensor gives opposite values for the weather loads.

Two different criteria for switching from the unberthing controller to the DP controller were tested for UNB2; SW1 and SW2. Without wind, the outcome is the same for SW1 and SW2, as the criteria are fulfilled at the same time. With wind forces applied, and without the wind feedforward control, the vessel is unable to unberth with SW2, while with SW1 the unberthing is fulfilled. As the unberthing force here is insufficient, switching to the DP controller is crucial to get enough force. For SW1 the switching to DP occurs soon enough for the vessel to be able to unberth, as the criteria is to switch when a desired distance from the quay is reached in *one* of the directions. For SW2, the desired position must be reached in both x- and y-directions, resulting in the switch never to happen, and the vessel is sliding against the quay in y-direction. However, when the vessel angle is kept constant throughout the unberthing, the vessel is able to unberth in both directions.

Neither of the switching criteria are optimal, as with SW1 the switching to DP happens when the vessel is still close to the quay in the x-direction, and with SW2 the vessel is far beyond the desired position in one of the directions, when the switching position is reached in the other, leading to huge oscillations. A solution would be to switch to DP separately in x- and y-direction to avoid the oscillatory behaviour. However, as the unberthing force is insufficient and the DP force here is needed for the vessel to unberth, switching to DP for x- and y- directions separately would not increase the vessel's ability to unberth.

Chapter 7

Conclusions and Further Work

The research questions of the thesis have been:

How can the docking process of a surface vessel be performed autonomously in a good manner? Is it possible to develop some unberthing control ensuring the vessel to leave the quay rapidly, to avoid the possibility of slamming against the quay upon leaving? Weather changes during the time the vessel is at quayside should be considered.

The following sections concludes how these questions have been answered and suggests how further developments can improve the outcome.

7.1 Concluding Remarks

To be able to perform docking of a surface vessel autonomously in a good manner, a hybrid control system was developed. As the need of different controllers in the docking scenario is based on the change of operation use mode during the docking, controllers for each operation use mode were designed. The switching between the controllers was performed by a supervisory switching logic and occurred in the transition between the operation modes. The operation modes considered are DP, berthing and quayside, unberthing, and back to DP.

Two different methods of unberthing were designed, tested and compared. The different methods have different qualities, advantages and disadvantages. Both methods gave rapidly unberthing and the vessel was able to avoid slamming against the quay upon leaving. A case-study was performed and the simulation results showed the necessity of implementing different algorithms; reset of the reference model and a wind feedforward control. The scenarios simulated in the case-study showed the vessel berthing and unberthing with and without resetting the reference model, and with and without wind loads applied.

7.2 Further Work

During the work of this thesis, several topics for further investigation have emerged, some of them are listed below.

- Machine learning of needed force for berthing and unberthing in various conditions. This is most relevant for ships often docking to the same quay, for example ferries.
- Implementing the hybrid control system designed in this thesis in a system for a fully autonomous vessel, including transit. Resetting of the system to be ready for a new round of docking would be necessary.
- Implement a quay-dependent weather force, for accuracy of the simulator. The weather loads acting on the vessel behave differently in open water and when the vessel is docked. The type of quay and tide could also be considered here.
- Expand the wind feeforward algorithm to be a weather feedforward algorithm, including wave and current loads. Additionally, the weather feedforward algortihm could be extended by altering the unberthing force dependent on the quay, tide and vessel. For instance small vessels are covered more by the quay than big vessels when it comes to wind from land. Thus small vessels need more unberthing force than huge vessels where the wind load is pushing the vessel out from quay.

Bibliography

Amarasinghe, D., Mann, G. K. I. & Gosine, R. G. (2005), 'Vision-based hybrid control strategy for autonomous docking of a mobile robot', *Proceedings of 2005 IEEE Conference on Control Applications, 2005. CCA 2005.* pp. 1600–1605.

Bitar, G. I. (2017), 'Towards the Development of Autonomous Ferries'.

Brodtkorb, A. H. (2017), Hybrid Control of Marine Vessels - Dynamic Positioning in Varying Conditions, PhD thesis, NTNU, Trondheim.

DNV GL (2018), 'The ReVolt'.
URL: *https://www.dnvgl.com/technology-innovation/revolt/index.html*

Fossen, T. I. (2011), *Handbook of Marine Craft Hydrodynamics and Motion Control [Bookshelf]*, Vol. 36, John Wiley & Sons.

Goebel, R., Sanfelice, R. G. & Teel, A. R. (2012), *Hybrid Dynamical Systems*, Princeton University Press.
URL: *https://www.jstor.org/stable/j.ctt7s02z*

Hassani, V., Sørensen, A. J., Pascoal, A. M. & Dong, N. T. (2012), 'Multiple model adaptive dynamic positioning', *IFAC Proceedings Volumes (IFAC-PapersOnline)* **9**(PART 1), 55–60.

Hespanha, J. (2001), 'Tutorial on supervisory control', *Lecture Notes for the workshop Control using Logic and Switching for the 40th Conf. on Decision and Contr.* pp. 1–46.

Hespanha, J. P., Liberzon, D. & Morse, A. S. (2003), 'Hysteresis-based switching algorithms for supervisory control of uncertain systems', *Automatica* **39**(2), 263–272.

Hespanha, J. P. & Morse, A. S. (2002), 'Switching between stabilizing controllers', *Automatica* **38**(11), 1905–1917.

Nguyen, T. D., Sørensen, A. J. & Tong Quek, S. (2007), 'Design of hybrid controller for dynamic positioning from calm to extreme sea conditions', *Automatica* **43**(5), 768–785.

Perez, T., Smogelif, N., Fossenf, T. I. & Sørensen, A. J. (2006), 'An overview of the marine systems simulator (MSS): A simulink® toolbox for marine control systems', *Modeling, Identification and Control* **27**(4), 259–275.

Rae, G., Smith, S., Anderson, D. & Shein, A. (1993), 'A Fuzzy Rule Based Docking Procedure for Two Moving Autonomous Underwater Vehicles', *1993 American Control Conference* pp. 580–584.

Rolls-Royce (2018), 'Rolls-Royce and Finferries demonstrate world's first Fully Autonomous Ferry'.
URL: *https://www.rolls-royce.com/media/press-releases/2018/03-12-2018-rr-and-finferries-demonstrate-worlds-first-fully-autonomous-ferry.aspx*

Skoglund, U. (2018), 'Førerløse ferger kan erstatte gangbruer - gemini.no'.
URL: *https://gemini.no/2018/06/forerlose-ferger-kan-erstatte-gangbruer/*

Sørensen, A. J. (2018), 'Marine Cybernetics : Towards Autonomous Marine Operations and Systems. Lecture Notes'.

Sørensen, A., Pedersen, E. & Smogeli, Ø. (2003), Simulation-based design and testing of dynamically positioned marine vessels, *in* 'Proc. of International Conference on Marine Simulation and Ship Maneuverability (MARSIM'03)'.

Steinsvik, I. L. (2019*a*), 'Information about docking', Personal Communication. Phone interview with Chief Mate I. L. Steinsvik on the manual docking process.

Steinsvik, J. L. (2019*b*), 'Information about docking of different ship types', Personal Communication. Phone interview with Chief Mate J. L. Steinsvik on the manual docking process.

Stensvold, T. (2017), 'Verdens første autonome skip i drift skal erstatte 40.000 vogntogturer i året - tu.no'.
URL: *https://www.tu.no/artikler/verdens-forste-autonome-skip-i-drift-skal-erstatte-40-000-vogntogturer-i-aret/382717*

Teo, K., Goh, B. & Chai, O. K. (2015), 'Fuzzy Docking Guidance Using Augmented Navigation System on an AUV', *IEEE Journal of Oceanic Engineering* **40**(2), 349–361.

Wärtsila Corporation (2018), 'World's first Autodocking installation successfully tested by Wärtsilä'.
URL: *https://www.wartsila.com/media/news/26-04-2018-world-s-first-autodocking-installation-successfully-tested-by-wartsila-2169290*

Appendices

A Description of MATLAB/Simulink MCSim 2019

This description was originally written by A. H. Brodtkorb for the 2018 version of MCSim. It is altered with the changes included by B. L. Steinsvik during the spring of 2019.

Below is a brief explanation of what the different files and modules in the MCSim 2019 contain. All subfolders must be added to the matlab path.

A.1 Initialisation files

InitBLS.m initialises the simulation. Here the chosen method for unberthing is set (Unb). The position of the quay, the time spent at quay and the desired vessel position for docking is decided under *Quay configuration*. The following files are called:

- **SimulationParameters:** sets parameters that are related to the environment, and enables/disables blocks. Here enabling/disabling the observer and controller are set.
- **Load_vessel_data:** loads the vessel data, currently Cybership 3 with updated model parameters.
- **ObserverParameters**: Sets observer parameters for the nonlinear passive observer. It also contains some other observer parameters below, but these are not included in the Simulink diagram.
- **SensorModule:** Adds noise and bias on measurements. The sensor module is enabled at the top of this file.
- **ControlParamters:** Sets the control parameters from the PID controller. P, I and D action can be enabled/disabled. The magnitude of the bias in the berthing controller is set here.
- **Log:** Enables/Disables vessel and sensor logging. The controller and observer settings are always logged within the "vessel controller" Simulink module.
- **ReferenceModel:** Sets parameters for the vessel model. The setpoints "pos_d1", "pos_unb" and "pos_d2" are added.

A.2 Simulink block diagram

In the Environment module waves, current, wind and ice time series are created. These are based on parameters from the SimulationParameters.m file. Within the Vessel module is where the vessel dynamics and controller live. The vessel module is displayed in Figure A.1 and the modules within are explained below.

Vessel Dynamics

This is where the vessel motion is calculated. It consists of a low-frequency (LF) part and a wave-frequency (WF) part, which are added to get the total vessel motion.

- Vessel WF 6 DOF: calculates the wave-frequency motion for N_wave number of wave components based on the motion transfer functions. The module is enabled/disabled from the SimulationParameters file.
- Vessel LF 6DOF: calculates the low-frequency vessel motion. (The model we use for control design is a simplified version of this model.)

Sensor module

Adds realistic values for sensor noise and bias. Measurements that are typically available on a ship:

- GNSS position (North, East) – a down measurement is also available, but is of lower quality
- Compass heading
- Gyrocompass angular rates (roll, pitch, yaw rates)
- IMU linear accelerations (surge, sway, heave accelerations)
- Wind sensor (wind direction and magnitude)

Vessel controller

Inputs: 6 DOF measured position, velocity, acceleration and wind (Eta_meas, Nu_meas, Acc_meas, Wind_meas), low-frequency position, velocity and acceleration (EtaLF, NuLF, AccLF), and the applied thrust (tau)
Outputs: Commanded thrust tau_c

- Nonlinear passive observer: model-based observer that estimates 3DOF (surge, sway, yaw) eta, nu and bias force.
- Controllers: Hybrid control is implemented with a DP controller, berthing controller, unberthing controller, supervisor and a switch. The controller module is shown in Figure A.2.
- Reference model: 3rd order filter
- Logging: sends parameters from the vessel controller to workspace for plotting

Comments about the inputs: The measurements can be down-sampled to more realistic sample rates by clicking the manual switch. When the observer is not used in closed loop, the low frequency states are used in the control law.

Thruster module

Contains first-order model that emulates that it takes some time before the commanded thrust is produced by the thrusters. There is no model of the thrusters in this version of MCSim.

Quay Module

Contains a step-function with a quayforce being $\approx$ infinty to avoid the vessel going beyond the quay. Rotation to the body-frame is implemented

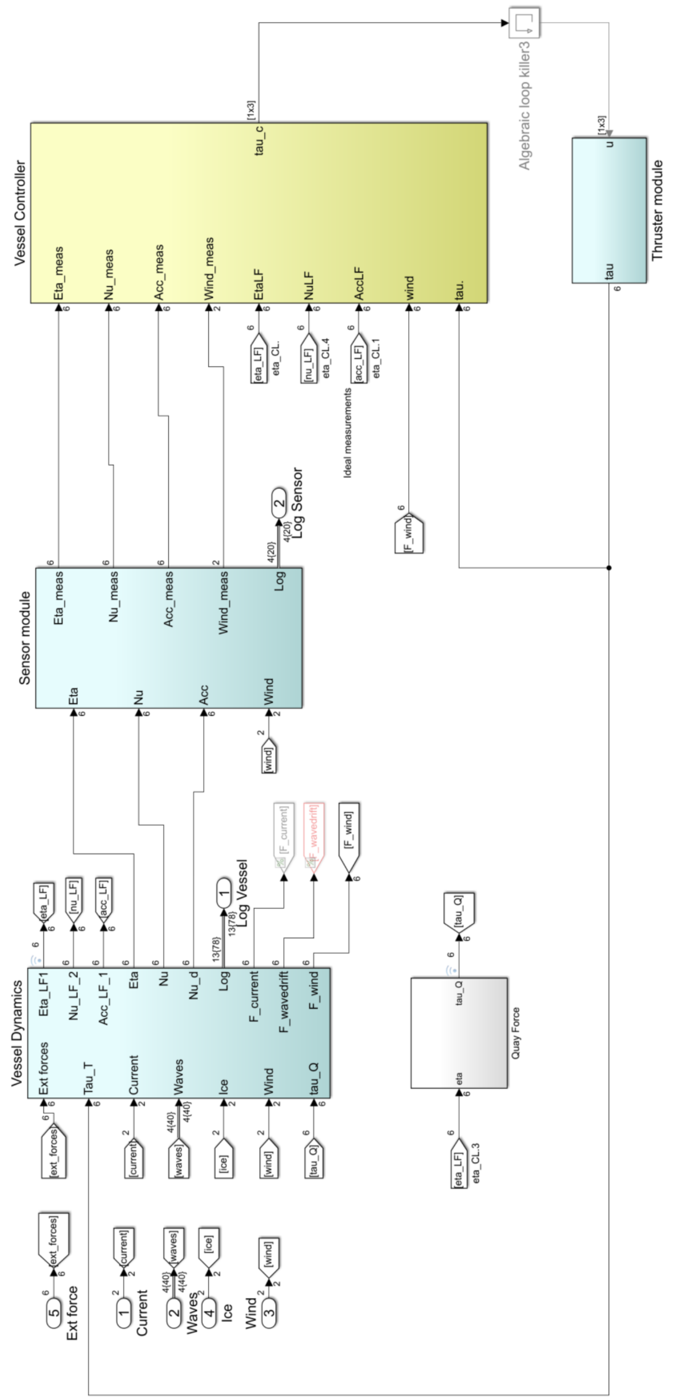

Figure A.1: Vessel module in MCSim. Showing the interaction between the vessel dynamics, sensor module, vessel controller, thruster module and quay module.

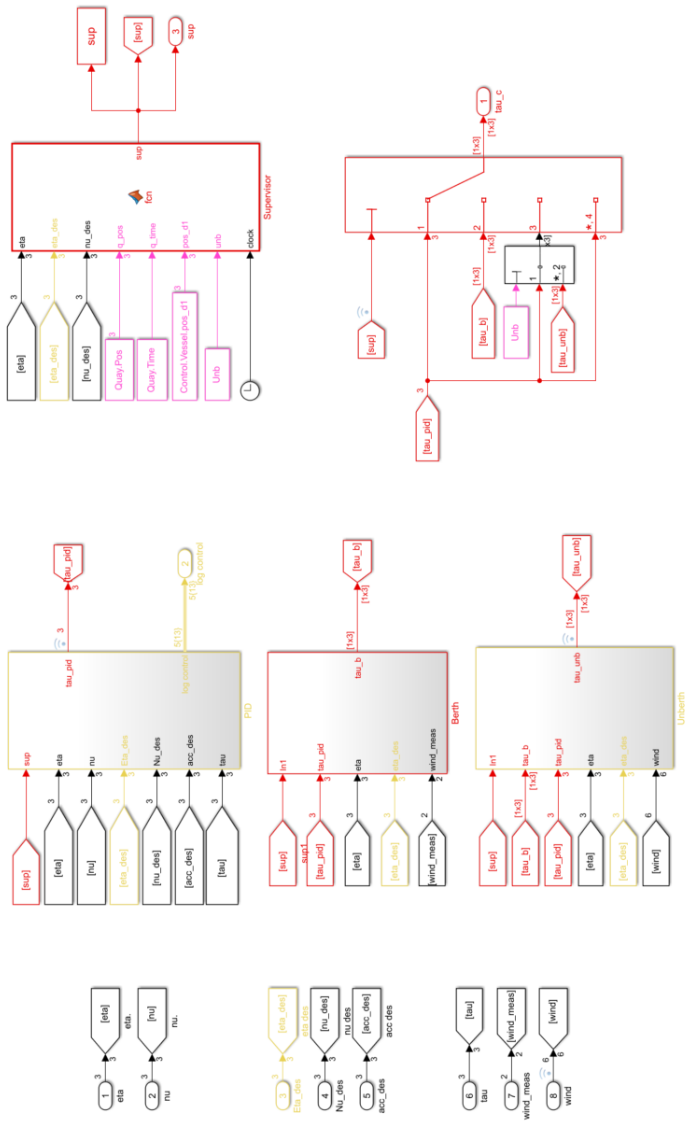

Figure A.2: Setup of the hybrid controller in Simulink. Displayed are the controllers for DP, berthing and unberthing in addition to the supervisor and the switch. The colors of the signals display the type of signal, where black is continuous, red is discrete, yellow is hybrid and pink is constant.

B Vessel Characteristics for Cybership 3

Table B.1: Principle hull data. (Brodtkorb 2017)

	Model-scale	Full-scale	
Length over all, L_{oa}	2.275	68.26	m
Length between perpendiculars, L_{pp}	1.971	59.13	m
Breadth moulded, B_m	0.437	13.11	m
Breadth waterline, B_{wl}	0.437	13.11	m
Draught at $L_{pp}/2, T$	0.153	4.59	m
Draught at fore perpendicular, T_{FP}	0.153	4.59	m
Draught at aft perpendicular, T_{AP}	0.153	4.59	m
Depth to main deck, D	0.203	6.10	m

Table B.2: Structure mass distribution. The original numbers from 1988 is given in parenthesis. AP is the aft perpendicular, BL is the baseline, CL is the centerline and CG is the center of gravity. (Brodtkorb 2017)

	Model-scale 2015 (1988)	Full-scale	
Mass	86.5 (74.7)	2 067 300	kg
Waterline	0.154 (0.153)	4.59	m rel. to BL
Trim	0.15 (0)	0	° rel. to BL
Longitudinal center of gravity, LCG	0.925 (1.005)	30.15	m rel. to AP
Transverse center of gravity, TCG	0 (0)	0	m rel. to CL
Vertical center of gravity, VCG	0.1105 (0.1956)	5.87	m rel. to BL
Roll moment of inertia, I_{44}	1.564 (2.192)	$58.74 * 10^6$	kgm^2
Pitch moment of inertia, I_{55}	18.939 (19.72)	$483.2 * 10^6$	kgm^2
Yaw moment of inertia, I_{66}	18.939 (19.72)	$483.2 * 10^6$	kgm^2
Roll radius of gyration, r_{44}	0.135 (0.1713)	5.139	m rel. to CG
Pitch radius of gyration, r_{55}	0.468 (0.5138)	15.41	m rel. to CG
Yaw radius of gyration, r_{66}	0.468 (0.5138)	15.41	m rel. to CG

NTNU

Norwegian University of
Science and Technology